Carbon dioxide effects of Antarctic stratification, North Atlantic Intermediate Water formation, and subantarctic nutrient drawdown during the last ice age: Diagnosis and synthesis in a geochemical box model

Mathis P. Hain,[1,2] Daniel M. Sigman,[1] and Gerald H. Haug[2,3]

Received 20 January 2010; revised 30 June 2010; accepted 27 July 2010; published 8 December 2010.

[1] In a box model synthesis of Southern Ocean and North Atlantic mechanisms for lowering CO_2 during ice ages, the CO_2 changes are parsed into their component geochemical causes, including the soft-tissue pump, the carbonate pump, and whole ocean alkalinity. When the mechanisms are applied together, their interactions greatly modify the net CO_2 change. Combining the Antarctic mechanisms (stratification, nutrient drawdown, and sea ice cover) within bounds set by observations decreases CO_2 by no more than 36 ppm, a drawdown that could be caused by any one of these mechanisms in isolation. However, these Antarctic changes reverse the CO_2 effect of the observed ice age shoaling of North Atlantic overturning: in isolation, the shoaling raises CO_2 by 16 ppm, but alongside the Antarctic changes, it lowers CO_2 by an additional 13 ppm, a 29 ppm synergy. The total CO_2 decrease does not reach 80 ppm, partly because Antarctic stratification, Antarctic sea ice cover, and the shoaling of North Atlantic overturning all strengthen the sequestration of alkalinity in the deepest ocean, which increases CO_2 both by itself and by decreasing whole ocean alkalinity. Increased nutrient consumption in the sub-Antarctic causes as much as an additional 35 ppm CO_2 decrease, interacting minimally with the other changes. With its inclusion, the lowest ice age CO_2 levels are within reach. These findings may bear on the two-stepped CO_2 decrease of the last ice age.

Citation: Hain, M. P., D. M. Sigman, and G. H. Haug (2010), Carbon dioxide effects of Antarctic stratification, North Atlantic Intermediate Water formation, and subantarctic nutrient drawdown during the last ice age: Diagnosis and synthesis in a geochemical box model, *Global Biogeochem. Cycles*, *24*, GB4023, doi:10.1029/2010GB003790.

1. Introduction

[2] Temporal variations of the atmospheric CO_2 mixing ratio have been reconstructed from air trapped in polar ice that accumulated over the late Pleistocene, providing a record that is astonishingly reminiscent of the glacial-interglacial climate cycles themselves (Figure 1) [*Petit et al.*, 1999]. Only the ocean carbon reservoir is adequately large and dynamic to drive the observed 80–100 ppm variations in atmospheric CO_2 on glacial-interglacial timescales. It is broadly suspected that the Southern Ocean is the key region of the ocean modulating these variations [e.g., *Sigman and Boyle*, 2000; *Sigman et al.*, 2010].

[3] The high sensitivity to Southern Ocean changes is fundamentally related to the tight grip it has on the efficiency of the "biological (or soft-tissue) pump", which sequesters carbon at depth by sinking organic matter, lowering atmospheric CO_2. Today, the Southern Ocean is the principal "leak" in the soft-tissue pump because its organic matter rain is inadequate to prevent the evasion of deeply sequestered carbon when deep water comes to its surface [*Sigman and Haug*, 2003; *Ito and Follows*, 2005; *Marinov et al.*, 2006; *Sigman et al.*, 2010]. Moreover, sequestration of carbon at depth lowers the pH of deep waters, making them more corrosive to sinking carbonate shells. This rain of $CaCO_3$, the "carbonate pump", delivers alkalinity to the deep ocean, which raises pH and makes deep waters less corrosive. Changing $CaCO_3$ saturation state, in turn, affects the depth of the lysocline; the depth level above which $CaCO_3$ is buried on the seafloor and alkalinity is lost from the ocean lowering "whole ocean alkalinity" [e.g., *Broecker and Peng*, 1987; *Boyle*, 1988b; *Sigman et al.*, 1998; *Toggweiler*, 1999; *Archer et al.*, 2000; *Sigman and Haug*, 2003; *Sigman et al.*, 2010]. These processes set atmospheric CO_2 on the timescales relevant to ice ages: more respired carbon (a stronger soft-tissue pump), less regenerated alkalinity (a weaker carbonate pump) and a

[1]Department of Geosciences, Princeton University, Princeton, New Jersey, USA.
[2]DFG-Leibniz Center for Surface Process and Climate Studies, Institut für Geowissenschaften, Universität Potsdam, Potsdam, Germany.
[3]Geologisches Institut, ETH Zurich, Zurich, Switzerland.

0886-6236/10/2010GB003790

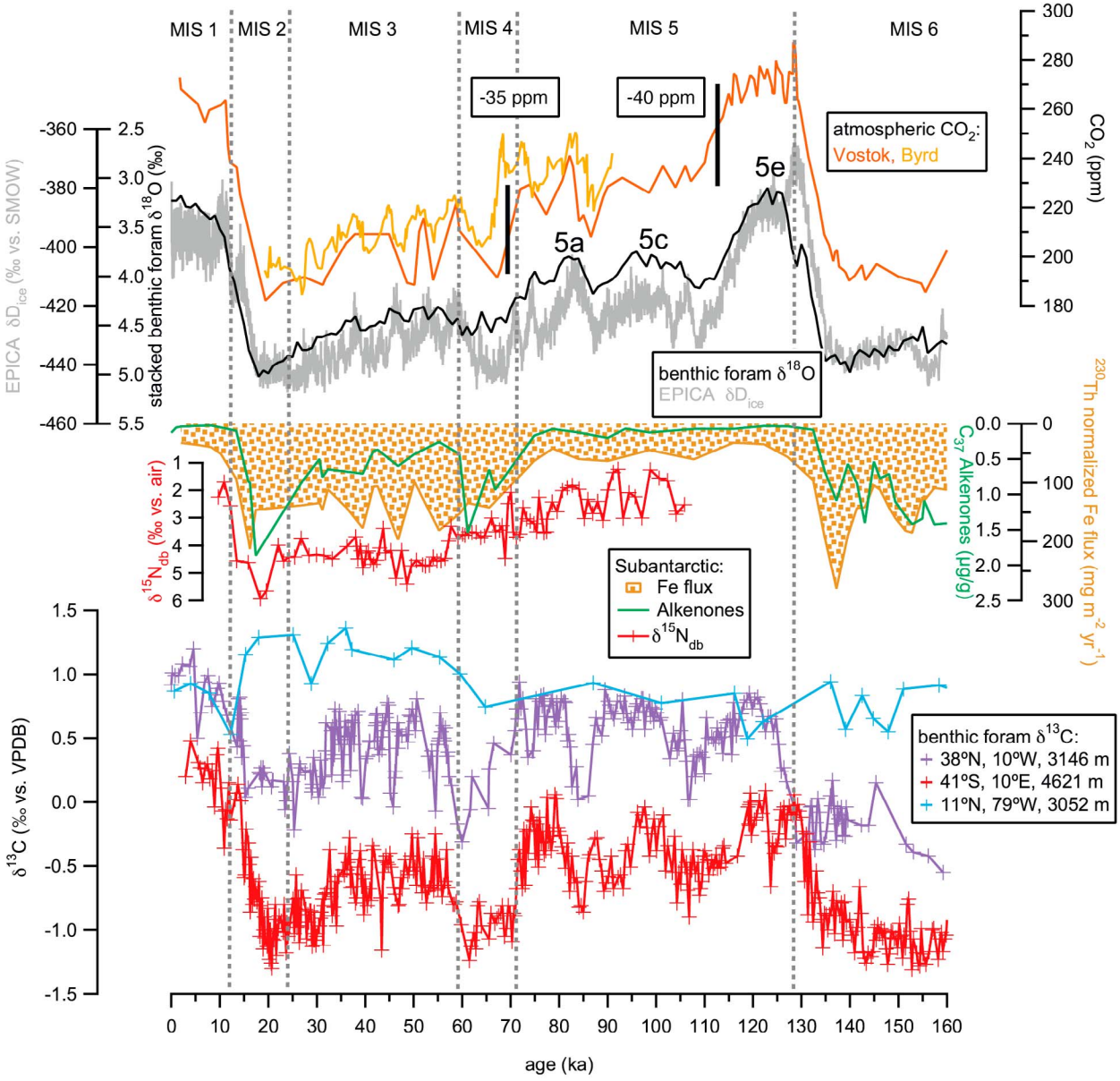

Figure 1. Atmospheric CO_2 over the last glacial cycle reconstructed from ice cores [*Petit et al.*, 1999; *Ahn and Brook*, 2008] and key proxy data related to the mechanisms driving its variability. A global stack of benthic foram $\delta^{18}O$ [*Lisiecki and Raymo*, 2005] reflecting both global ice volume and deep ocean temperatures illustrates the close relationship between atmospheric CO_2 and the glacial cycle. The temporal correlation between the first major decrease of CO_2 during Marine Isotope Stage (MIS) 5 and rapid Antarctic cooling (EPICA δD) [*Petit et al.*, 1999] may indicate an important role for the onset of Antarctic stratification and/or sea ice expansion. During MIS 4, 3, and 2, aeolian iron supply, productivity (Alkenones) [*Martinez-Garcia et al.*, 2009], and nutrient consumption (as reconstructed from diatom-bound $\delta^{15}N$, $\delta^{15}N_{db}$ [*R. S. Robinson et al.*, 2005]) increased in the sub-Antarctic. During MIS 4, 3, and 2, the benthic forminiferal $\delta^{13}C$ at two sites currently bathed by NADW decreased (purple and red) [*Shackleton et al.*, 2000; *Hodell et al.*, 2003], while $\delta^{13}C$ increased at a Carribbean site that monitors intermediate-depth Atlantic waters (blue) [*Oppo et al.*, 1995]. These collective observations fit into the widespread evidence for a shoaling of North Atlantic overturning (from NADW to GNAIW) [*Lynch-Stieglitz et al.*, 2007]. The fertilization of the sub-Antarctic and/or the formation of GNAIW may have been important contributors to the second major decrease in atmospheric CO_2 at the MIS 4/5 transition.

higher whole ocean alkalinity all act to partition CO_2 from the atmosphere into the ocean.

[4] Using a geochemical ocean/atmosphere box model, we systematically probe and analyze the most promising oceanographic hypothesis for the low levels of CO_2 during ice ages: (1) polar Antarctic stratification and sea ice expansion restricting air-sea gas exchange, (2) polar Antarctic nutrient drawdown, (3) shoaling of North Atlantic overturning, and (4) subantarctic nutrient drawdown. A new diagnostic tool quantitatively parses simulated CO_2 change into its component geochemical causes (see above), providing mechanistic insight into how these ocean changes operate to influence atmosphere chemistry. This exercise reveals a new dynamic involving the carbonate pump, which reduces the leverage of the polar Antarctic "barrier mechanisms", stratification and sea ice expansion, and thus renders the other ocean changes relatively more important. The central outcome of this study, however, is the surprising magnitude of interactions among the oceanographic hypotheses for glacial CO_2 drawdown. These interactions, which to this point have not been characterized, greatly affect the CO_2 drawdown that can be achieved.

[5] Below, before discussing our model simulations, we provide more information and constraints on the hypotheses we set out to investigate.

1.1. Antarctic

[6] The Antarctic is arguably a more important contributor to the Southern Ocean leak in the soft-tissue pump than the subantarctic zone because (1) it ventilates the voluminous deep rather then the smaller-volume mid-depth ocean (e.g., that ventilated by subantarctic mode water) and (2) its concentration of "preformed" nutrients carried into the ocean interior together with the water instead of sinking organic matter is much greater [*Marinov et al.*, 2006]. Accordingly, hypotheses have focused on closing the Antarctic component of the Southern Ocean leak in the soft-tissue pump. First, nutrient consumption in the Antarctic surface may have increased [*Sarmiento and Toggweiler*, 1984; *Martin*, 1990; *François et al.*, 1997]. Second, reduced exchange between the Antarctic surface and the underlying ocean may have decreased the rate of exposure of CO_2 charged deep water (often summarized as "stratification") [*François et al.*, 1997; *Toggweiler*, 1999]. Third, extensive sea ice cover may have prevented evasion of CO_2 during the glacial [*Stephens and Keeling*, 2000]. In the polar Antarctic, which ventilates the deep ocean, stratification and gas-exchange reduction, when taken to completion, have equivalent capacities to lower CO_2 and may collectively be called "barrier mechanisms" [*Archer et al.*, 2003].

[7] Antarctic export production appears to have been reduced during ice ages [*François et al.*, 1997; *Frank et al.*, 2000; *Kumar et al.*, 1993; *Mortlock et al.*, 1991; *Kohfeld et al.*, 2005], arguing against a simple productivity-driven increase in nutrient consumption. If, however, gross nutrient supply to the Antarctic surface decreased as export production decreased (and especially if the nutrient supply decreased more), atmospheric CO_2 might have been lowered without violating the apparent productivity constraint. Unfortunately, the parameter of singular importance, the surface nutrient status of the ice age Antarctic, is debated [e.g., *Keigwin and Boyle*, 1989; *De La Rocha et al.*, 1998; *De La Rocha*, 2006; *Sigman et al.*, 1999; *Elderfield and Rickaby*, 2000; *Crosta and Shemesh*, 2002; *Robinson et al.*, 2004; *Robinson and Sigman*, 2008].

[8] Previous studies have been taken to indicate that substantial fractions of the ice age CO_2 drawdown can be driven by either of the two Antarctic barrier mechanisms (reducing Antarctic overturning [*Toggweiler*, 1999]; reduced Antarctic CO_2 efflux by sea ice cover [*Stephens and Keeling*, 2000]), This raises the question of whether the barrier mechanisms could be combined to explain the entire CO_2 drawdown. If so, nutrient status and non-Antarctic mechanisms would be relegated to a role of secondary importance. Below, we will show that the carbonate pump reduces the sensitivity of CO_2 to the barrier mechanisms, and we will argue that the studies above underestimate its importance. We also show that the three proposed Antarctic mechanisms, when combined, can achieve little more CO_2 drawdown than any one of them in isolation. This motivates inclusion of other oceanographic changes and their interaction with the Antarctic mechanisms.

1.2. Shoaling of North Atlantic Overturning

[9] During parts of the last glacial cycle, the conversion from deep (NADW) to intermediate (GNAIW) water formation in the North Atlantic left the abyssal Atlantic dominated by southern sourced water (possibly akin to modern Antarctic Bottom Water; AABW) [*Boyle and Keigwin*, 1982; *Duplessy, et al.*, 1984, 1988; *Boyle*, 1988a; *Yu et al.*, 1996; *Marchitto et al.*, 2002; *McManus et al.*, 2004; *Curry and Oppo*, 2005; *L. F. Robinson et al.*, 2005; *Gherardi et al.*, 2009]. This may have contributed to the development of an apparent "chemical divide" at ~2–2.5 km depth in the ice age ocean, best documented for the Atlantic [e.g., *Lynch-Stieglitz et al.*, 2007] but also evident from some data in the Indo-Pacific [*Kallel et al.*, 1988; *Herguera*, 1992; *Boyle et al.*, 1995; *Keigwin*, 1998; *Matsumoto and Lynch Stieglitz*, 1999; *Matsumoto et al.*, 2002; *Galbraith et al.*, 2007]. The "NADW-to-GNAIW switch" has been proposed to isolate the ocean's deepest waters, making them prone to the accumulation of nutrients and excess carbon, as is supported by paleoceanographic data [*Boyle and Keigwin*, 1987; *Boyle et al.*, 1995; *Duplessy et al.*, 1988; *Kallel et al.*, 1988].

[10] The NADW-to-GNAIW switch may help Antarctic hypotheses for CO_2 change in two ways. First, it supports the Antarctic stratification hypothesis (see above) in the sense that, even with reduced Antarctic overturning during ice ages, southern sourced waters might have filled a larger volume of the abyssal ocean than observed during interglacials; in this way, it helps to match observations. Second, the focusing of respired carbon in the abyssal ocean, as opposed to mid-depths, would have made the waters overlying the lysocline more corrosive, raising whole ocean alkalinity and further lowering CO_2 levels [*Boyle*, 1988a, 1988b].

[11] However, an opposing CO_2 effect of the NADW-to-GNAIW switch, operating through the soft-tissue pump, would work to raise CO_2 during ice ages: Relative to NADW and its downstream forms, modern AABW has a large burden of preformed nutrients. If abyssal depths of all the glacial ocean basins were occupied by AABW with near its present-day burden of preformed nutrients (as opposed to regenerated nutrients from sinking organic matter), the increase in volumetric importance of AABW would have driven higher, not lower, atmospheric CO_2 [e.g., *Marinov et al.*, 2008]. Understanding how these different carbon cycle aspects interact to yield a net CO_2 effect from the NADW-to-GNAIW switch, under various Southern Ocean conditions, is the second goal of this study.

1.3. Subantarctic Nutrient Drawdown

[12] The subantarctic zone (SAZ) of the Southern Ocean, unlike the Antarctic, was more productive during the last ice age, and nutrient consumption may also have been greater than is observed today [*Kumar et al.*, 1995; *Mashiotta et al.*, 1997; *Rosenthal et al.*, 1997, 2000; *R. S. Robinson et al.*, 2005; *Kohfeld et al.*, 2005; *Robinson and Sigman*, 2008; *Martinez-Garcia et al.*, 2009], perhaps explained by natural iron fertilization of the region by dust during parts of the last and previous ice ages [*Watson et al.*, 2000; *Martinez-Garcia et al.*, 2009]. As a result, a number of workers have pointed to its potential role in explaining the low CO_2 of ice ages [e.g., *Watson et al.*, 2000; *R. S. Robinson et al.*, 2005; *Matsumoto and Sarmiento*, 2008].

[13] The subantarctic zone ventilates a smaller volume of the ocean interior than does the Antarctic. Thus, its control on the biological pump should be limited. However, the subantarctic zone is the gate keeper for nutrients attempting to pass from the Southern Ocean into the mid-depth ocean of the low latitudes where they fuel biogenic fluxes out of the low-latitude surface ocean [*Toggweiler et al.*, 1991; *Sarmiento et al.*, 2004]. As a result, it may affect the carbon cycle through a number of processes involving ocean alkalinity [*Keir*, 1988]. First, more complete nutrient consumption in the SAZ should work to keep regenerated nutrients and respired CO_2 in the deep (rather than mid-depth) ocean, where it can transiently shoal the lysocline and force a rise in whole ocean alkalinity. Second, by reducing the nutrient supply to the lower latitudes, SAZ nutrient depletion may work to lower the rain of $CaCO_3$ out of low-latitude ocean [e.g., *Matsumoto et al.*, 2002; *Loubere et al.*, 2004; *Matsumoto and Sarmiento*, 2008], which would drive the ocean to deepen its steady state lysocline to balance the river input of alkalinity, further raising whole ocean alkalinity [*Sigman et al.*, 1998]. Third, muted $CaCO_3$ rain would reduce the amount of regenerated alkalinity found in the ocean interior at any given time; a weakened carbonate pump.

[14] Our model can differentiate subantarctic and Antarctic processes (see below) allowing us to probe subantarctic fertilization for its isolated CO_2 drawdown capacity as well as its interactions with the Antarctic and North Atlantic mechanisms discussed above. In particular, *Watson et al.* [2000] have simulated that iron fertilization applied to the entire Southern Ocean in the context of an interglacial background state may explain the component of atmospheric CO_2 decline that correlates to enhanced dust supply to the region (Figure 1). The third goal of our study is to answer if subantarctic (rather than Southern Ocean) nutrient status, in the context of the Antarctic mechanisms and the NADW-to-GNAIW switch, maintains the same effect on CO_2.

2. Model Description

[15] We employ the CYCLOPS biogeochemical box model [*Keir*, 1988] with the addition of (1) a dynamical lysocline [*Sigman et al.*, 1998], (2) a subantarctic zone (SAZ) surface box [*R. S. Robinson et al.*, 2005], and (3) a polar Antarctic zone (PAZ) box representing the surface between the Antarctic polar front and the continental margin [*Sigman et al.*, 2009]. This model geometry allows for consideration of the different productivity changes observed in these component regions of the Southern Ocean [e.g., *Mortlock et al.*, 1991; *Frank et al.*, 2000; *Kohfeld et al.*, 2005; *Martinez-Garcia et al.*, 2009] and spatially separates upper and lower cell biogeochemical dynamics [*Toggweiler*, 1999; *Marinov et al.*, 2006].

[16] As noted above, we carry out "stratification" experiments by varying two aspects of the polar Antarctic. First, the rate of mixing between the polar Antarctic zone surface (PAZ box) and the circumpolar deep water (CDW box) below is varied between 20 and 0.1 Sv. Second, we vary the surface nutrient concentration in the PAZ from the standard value of 2 down to 0 μM of $[PO_4^{3-}]$. From the standard interglacial case, this effectively increases PAZ nutrient consumption, that is, the fraction of gross nutrient supply being utilized for export production.

[17] To address apparent changes between interglacial and glacial hydrography, we construct a "glacial" circulation pattern characterized by (1) the formation of intermediate depth water in the North Atlantic (GNAIW circulation) (similar to the circulation schemes explored by *Sigman et al.* [2003]) and (2) upwelling of intermediate depth water rather then CDW into the open Antarctic surface (Figure 2).

Figure 2. An altered version of the CYCLOPS geochemical box model [*Keir*, 1988], model architecture, and two circulation schemes ((a) NADW- and (b) GNAIW-associated) used in the model experiments. Arrows linking boxes denote transports of water, in Sverdrups (Sv, 10^6 m^3s^{-1}). The main differences between the two circulation schemes are (1) the depth of North Atlantic ventilation and (2) the subsurface source of wind-driven upwelling in the Southern Ocean; see "cartoon" insets. The rain of organic matter and $CaCO_3$ from the surface is shown in gray; the numbers indicate the fractions delivered to each downstream box, respectively, and C_{org}:$CaCO_3$ remineralization ratios. $CaCO_3$ is only produced in the low-latitude surface boxes. Some of the carbonate rain reaching the deep boxes is buried on the seafloor above the lysocline, following the parameterization of *Sigman et al.* [1998]. All surface boxes exchange CO_2 with a well-mixed atmosphere.

[18] More efficient nutrient consumption in the subantarctic zone of the Southern Ocean is simulated by a reduction of surface $[PO_4^{3-}]$ concentrations in our SAZ box from 1.2 μM in the reference to 0.7 μM, as adopted from *R. S. Robinson et al.* [2005]. This change is conducted in the context of both NADW- and GNAIW-circulation.

[19] In CYCLOPS, the high-latitude surface boxes (all Southern Ocean boxes as well as the North Atlantic) are

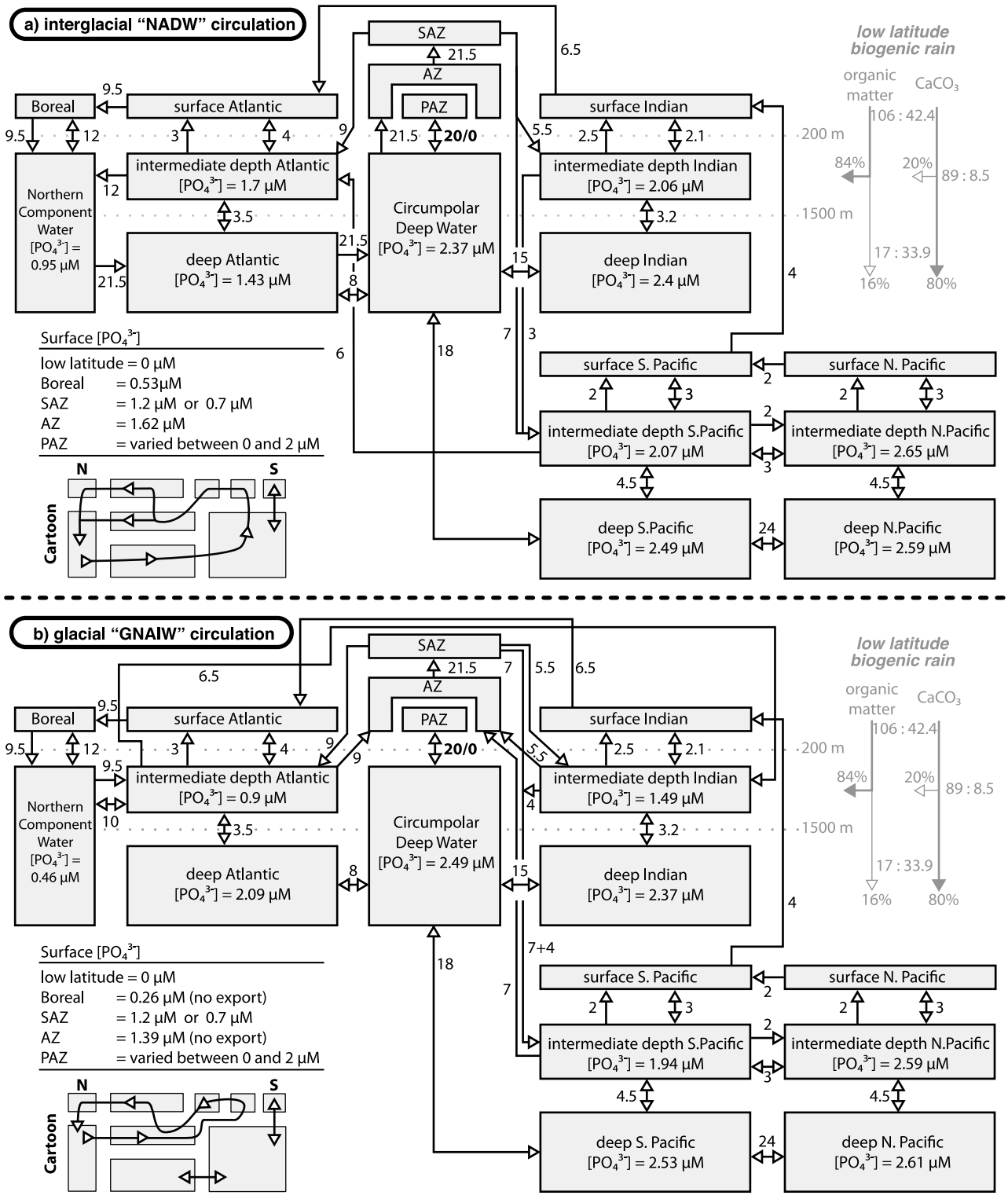

Figure 2

Table 1. Summary of Model Experiments Conducted

Experiment	Circulation	Subantarctic $[PO_4^{3-}]$ (μM)	Polar Antarctic $[PO_4^{3-}]$ (μM)	Polar Antarctic Overturning (Sv)	Polar Antarctic Piston Velocity (%)	Figure
Interglacial reference	NADW	1.22	2	20	100	3
Stratification	NADW	1.22	2 to 0	20 to 0.1	100	3
GNAIW	GNAIW	1.22	2 to 0	20 to 0.1	100	4
SAZ	NADW	0.7	2 to 0	20 to 0.1	100	5
GNAIW+SAZ	GNAIW	0.7	2 to 0	20 to 0.1	100	6
Sea ice	NADW	1.22	2 to 0	20	0 to 100	S2

assumed not to produce a $CaCO_3$ rain [*Keir*, 1988]. For the export out of the low-latitude surface boxes, at a depth of 200 m, we follow the original CYCLOPS $CaCO_3/C_{org}$ rain ratio of 0.4 [*Keir*, 1988]. This value is higher than estimated from vertical ocean gradients [*Sarmiento et al.*, 2002], data-driven model optimization [*Kwon and Primeau*, 2008] and than used in other box models [e.g., *Toggweiler*, 1999; *Stephens and Keeling*, 2000; *Köhler et al.*, 2005; *Peacock et al.*, 2006]. However, the high rain ratio of 0.4 in conjunction with our mid-depth $CaCO_3/C_{org}$ regeneration ratio of ~0.1 [*Anderson and Sarmiento*, 1994] (Figure 2) results in particulate rain to the deep boxes with a $CaCO_3/C_{org}$ ratio of 2, which broadly agrees with sediment trap data of the deep ocean [*Klaas and Archer*, 2002]. If one were to use the proposed export rain ratio of < 0.1 [*Sarmiento et al.*, 2002; *Kwon and Primeau*, 2008] along with a mid-depth $CaCO_3/C_{org}$ regeneration ratio of ~0.1 [*Anderson and Sarmiento*, 1994] and a typical organic carbon regeneration profile [e.g., *Berelson*, 2001], then none of the $CaCO_3$ sinking out of the surface ocean would reach the deep seabed, and the model's ocean $CaCO_3$ budget could not simulate observed conditions. Further, our choice of export rain ratio gives rise to 69 μM ocean average alkalinity regenerated from $CaCO_3$ and thus a carbonate pump of observed strength (see discussion). To address the concern that the distribution of $CaCO_3$ rain greatly affects our results, we apply an alternative rain ratio scheme that partitions a portion of the $CaCO_3$ rain from low to high latitudes (Table S1 and Figure S1).[1] This sensitivity test has no significant effect on the Antarctic mechanisms. There are second-order impacts on the CO_2 effects of the NADW-to-GNAIW switch and subantarctic nutrient drawdown, but these changes largely cancel one another.

[20] We employ a globally constant temperature and salinity (5°C, 34.7 psu). This treatment of the solubility pump [e.g., *Toggweiler et al.* 2003], the effect of water temperature on CO_2 solubility, is simple and flawed. We deliberately choose to simulate an "isothermal" ocean to make our model experiments directly comparable, eliminating the need to correct for temperature changes when assessing the geochemical impact on CO_2. The effect of ocean cooling (ΔpCO_2 ~−30 ppm, [*Sigman and Boyle*, 2000]) appears to be countered by other changes, such as the contraction of the terrestrial biosphere, the effect of higher ocean salinity (ΔpCO_2~+15 ppm; $\Delta\, pCO_2$~+6.5 ppm) [*Sigman and Boyle*, 2000], and the reduction in ocean volume (+8 ppm) [*Brovkin et al.*, 2007].

[21] Finally, we conduct an experiment in which, rather than decreasing PAZ/deep water exchange, we reduce the CO_2 air/sea gas-exchange rate of the PAZ box, as a simple way to assess the geochemical potential to reduce ice age atmospheric CO_2 by increased sea ice cover [*Stephens and Keeling*, 2000]. This gas-exchange experiment, which is reported only in the context of the NADW circulation, allows for comparison with the CO_2 effects of PAZ "stratification". All of our experiments are summarized in Table 1.

[22] The reference for our experiments below is the model's representation of the present interglacial state of the ocean. This state is characterized by an atmospheric CO_2 mixing ratio of 270.4 ppm (Figures 3a, 4a, 5a, and 6a show the deviation from this reference value). If gas exchange were infinite in this reference case, some deeply sequestered CO_2 could evade, in particular from the PAZ, and atmospheric CO_2 would be ~2 ppm higher (upper right corner in Figure 3b). Moreover, in all of our experiments, we isolate the CO_2 effects of the soft-tissue pump, the carbonate pump (internal carbonate cycle) and whole ocean alkalinity (open system carbonate cycle) as well as their interaction. A brief description of the separation technique is in the online supporting information (Text S1).

3. Model Results

[23] Before assessing plausible glacial parameter combinations, we describe the dominant dynamics that arise throughout our experiments (Figures 3, 4, 5, and 6), an exercise that also clarifies the separation of geochemical components used herein.

[24] First, P*, the fraction of ocean $[PO_4^{3-}]$ that is regenerated, describes the efficiency of the soft-tissue pump, either with respect to a given deep ocean ventilation pathway or the global ocean [*Ito and Follows*, 2005]. When the fraction of unutilized $[PO_4^{3-}]$ in the PAZ surface (i.e., $[PO_4^{3-}]_{PAZ}/[PO_4^{3-}]_{CDW}$) equals the 1-P* of CDW, the global ocean P* (and thus the global soft-tissue pump) becomes insensitive to the simulated changes in PAZ/CDW mixing (dashed line "P" in Figures 3 to 6).

[25] Second, as PAZ/CDW mixing approaches zero, the PAZ is effectively not participating in ocean dynamics (i.e., it is not ventilating the ocean interior, Figure 7). Thus, the

[1] Auxiliary materials are available with the HTML. doi:10.1029/2010GB003790.

ocean carbon cycle and atmospheric CO_2 become insensitive to PAZ nutrient status (along the left edge of the panels in Figures 3, 4, 5, and 6). This is also true for complete sea ice cover of the PAZ (Figure S1).

[26] Third, in contrast to the soft-tissue pump (panels d and g in Figures 3, 4, 5, and 6), the carbonate pump (panel f) as represented by regenerated alkalinity from carbonate dissolution at depth (panel i) is primarily influenced by PAZ/CDW mixing, not PAZ nutrient status, because (1) export production in the PAZ is not associated with a $CaCO_3$ rain in our model, consistent with observations [*Honjo*, 2004], and (2) the ventilation of abyssal water in the PAZ is the most direct conduit through which regenerated alkalinity surfaces and takes up CO_2 from the atmosphere (i.e., transforms into preformed alkalinity). Thus, the ventilation of deep waters in the Southern Ocean represents an important leak in the global carbonate pump that, in contrast to the leak in the soft-tissue pump, lowers atmospheric CO_2 [cf. *Broecker and Peng*, 1989].

[27] Fourth, having isolated these two geochemical components, the soft-tissue and carbonate pumps, it becomes clear that whole ocean alkalinity amplifies their combined

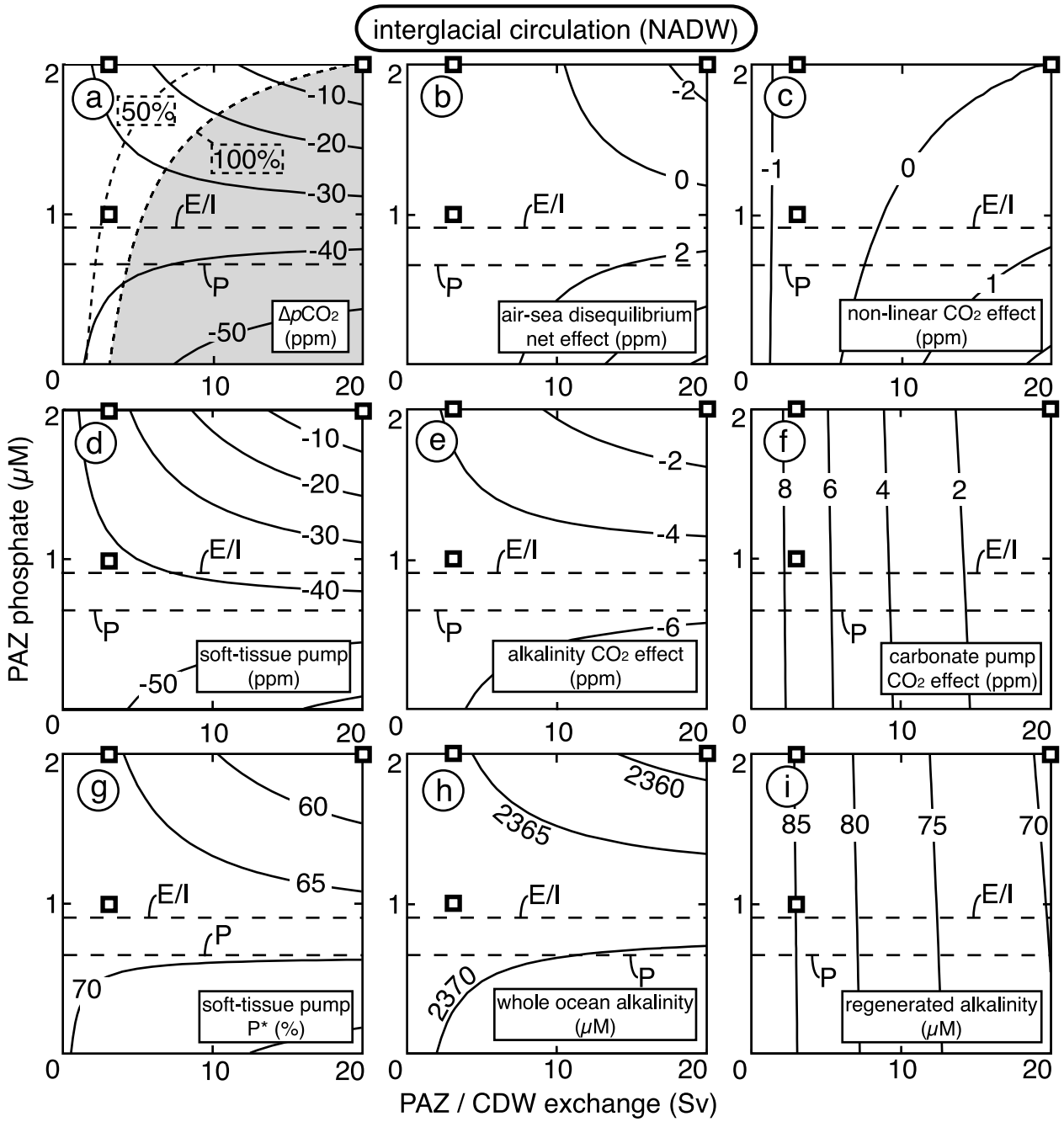

Figure 3

CO_2 effect in a surprisingly simple way. To demonstrate this, we plot the whole ocean alkalinity component of simulated CO_2 change versus the sum of all other components (i.e., "closed system") (Figure 8). All model runs within a given experiment fall onto a common trend, while each experiment occupies a unique region in the plot. The trends within each experiment are roughly linear, and their slope varies as a function of the background global ocean circulation (1/6 and 1/3 with the NADW- and GNAIW-associated circulation, respectively; Figure 8). Hence, the open system $CaCO_3$ cycle amplifies polar Antarctic–driven CO_2 changes by a factor 1.16 (NADW) or 1.32 (GNAIW). In detail, whole ocean alkalinity change amplifies each of the other major geochemical components: a more efficient soft-tissue pump, a sea ice–driven reduction in PAZ CO_2 evasion (i.e., the air-sea disequilibrium component; Figure 8, gray markers), and a stratification-strengthened carbonate pump (amplifying the effect of this component to raise CO_2). The stronger amplification of the PAZ-driven changes under the GNAIW circulation (i.e., the greater slope in Figure 8) results from the greater fraction of the deep ocean ventilated by the PAZ in the GNAIW case, so that the polar Antarctic exerts a stronger control on deep ocean $[CO_3^{2-}]$. The overall greater range on the *x* axis of the GNAIW experiments in Figure 8 also results from the expanded volume of PAZ ventilation in the GNAIW case, which lends more CO_2 leverage to PAZ surface nutrient concentration.

[28] Fifth, the consistent offset toward greater whole ocean alkalinity-driven CO_2 drawdown in the experiments with GNAIW formation and/or subantarctic (SAZ) fertilization (Figure 8; vertical offset among experiments) is largely caused by "nutrient deepening" [*Boyle*, 1988a, 1988b], through two mechanisms: (1) respired carbon is focused at the depth of the lysocline, causing a dissolution event (i.e., transient lysocline shoaling), and (2) there is a decline in low-latitude productivity and thus $CaCO_3$ rain (Table 2), causing the steady state lysocline to deepen [*Sigman et al.*, 1998]. In addition, specific to the NADW-to-GNAIW switch, the incursion of corrosive Indo-Pacific deep water into the Atlantic basin causes a dissolution event there [*Emerson and Archer*, 1992].

[29] Sixth, at the particular degree of PAZ nutrient consumption at which the opposing sensitivities of the soft-tissue pump and the carbonate pump exactly cancel one another, there is no change in the partitioning of CO_2 between the atmosphere and ocean as PAZ/CDW mixing and sea ice cover change (dashed line labeled "E/I" in Figures 3, 4, 5, and 6). At this degree of nutrient consumption, PAZ pCO_2(aq) must equal atmospheric CO_2, with CO_2 evasion (E) above and invasion (I) below. Along the E/I line, deep ocean $[CO_3^{2-}]$ can also not change, so lysocline depth and whole ocean alkalinity remain constant in the face of the changing strength of a PAZ barrier to air-sea CO_2 exchange (Figures 3e, 4e, 5e, and 6e). Below the E/I line, PAZ stratification and sea ice cover act to raise atmospheric CO_2.

3.1. PAZ Changes Under Interglacial Circulation

3.1.1. PAZ Nutrient Drawdown

[30] In the context of the interglacial (NADW-based) circulation, a maximal drawdown of atmospheric CO_2 is achieved by an enhancement of nutrient consumption in the PAZ while keeping mixing at the interglacial control value of 20 Sv (following the right edge of the panels in Figure 3). This transforms the PAZ box from the least efficient end-member in terms of soft-tissue pump to being as efficient as the low-latitude surface ocean, leading to a strong increase in the fraction of regenerated nutrients in the ocean (Figure 3d) [*Sigman and Haug*, 2003; *Ito and Follows*, 2005; *Marinov et al.*, 2008]. Moreover, the additional carbon released by respiration in the ocean interior decreases the carbonate ion concentration ($[CO_3^{2-}]$), causing a dissolution event that increases whole ocean alkalinity (Figure 3e) until $[CO_3^{2-}]$ is restored and the alkalinity budget of the ocean comes back into balance [*Sigman et al.* 1998]. The net atmospheric CO_2 decline is 58 ppm (Figure 3a), dominated by the soft-tissue pump ($\Delta pCO_2 = -62$ ppm; Figure 3d) and whole ocean alkalinity ($\Delta pCO_2 = -8$ ppm; Figure 3e). The carbonate pump (Figures 3f and 3i) is not a factor in this scenario. At a

Figure 3. Model results for the polar Antarctic zone stratification experiment, conducted with interglacial-like "NADW circulation" (see section 3.1). The parameters PAZ/CDW mixing and PAZ nutrient status are varied systematically from 0.1 to 20 Sv and 0 to 2 μM $[PO_4^{3-}]$, respectively. (a) The simulated difference atmospheric CO_2 partial pressure from the interglacial reference case (upper right corner of each panel). From three prognostic parameters, (g) the ocean average fraction of regenerated $[PO_4^{3-}]$, (h) whole ocean alkalinity, and (i) alkalinity regenerated by carbonate dissolution at depth, we calculate the (d) isolated impact on atmospheric CO_2 of the soft-tissue pump, (e) whole ocean alkalinity, and (f) carbonate pump. (b) The CO_2 difference relative to a hypothetical case of complete equilibration between the surface ocean and atmosphere; if negative, incomplete equilibration lowers CO_2. The above components also affect one another to yield (c) a nonlinear component of CO_2 change (see Text S1), which is small in this case. Note that the carbonate pump (Figure 3g) depends almost entirely on PAZ overturning because export production in the PAZ is not associated with $CaCO_3$. The horizontal lines labeled "E/I" mark the PAZ nutrient status at which PAZ pCO_2 equals the atmospheric pCO_2 while the horizontal lines labeled "P" mark the nutrient status at which the fraction of regenerated nutrients in the CDW equals the fraction of nutrients utilized in the PAZ. Along these horizontal lines, atmospheric CO_2 (Figure 3a) and the soft-tissue pump (Figure 3g), respectively, become insensitive to PAZ overturning. The two short-dashed curves indicate PAZ productivity that is 50% and 100% of the interglacial reference case (upper right corner). The bold squares highlight model runs shown in Table 2.

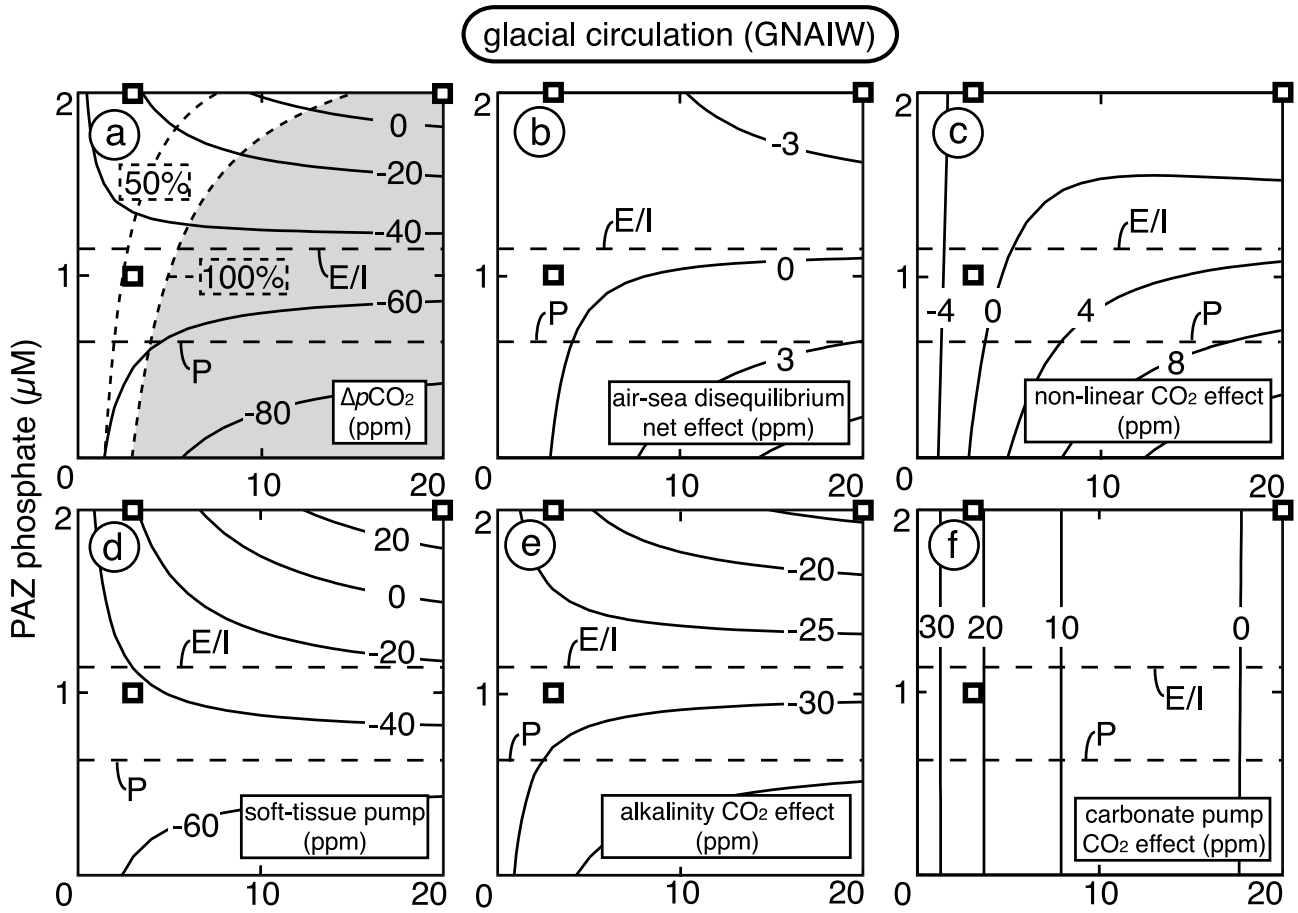

Figure 4. Model results for the polar Antarctic zone stratification experiment, conducted with glacial-like "GNAIW circulation" (see section 3.2; for description, see Figure 3). The fraction of regenerated nutrients, whole ocean and regenerated alkalinity concentration can be found in Figure S3. Note that the CO_2 change associated with (d) the soft-tissue pump, (e) whole ocean alkalinity, (f) carbonate pump, (c) nonlinear effect, and the productivity constraints (curves labeled 50% and 100%) are all relative to the interglacial reference (upper right corner in Figure 3).

surface [PO_4^{3-}] of ~0.9 μM, the PAZ switches from a region of CO_2 evasion to one of invasion (below "E/I" in Figure 3), which reverses the net CO_2 effect of air-sea gas-exchange limitation from −2 ppm CO_2 in the standard interglacial case to +6 ppm such that infinite gas exchange would have yielded an 8 ppm greater CO_2 drawdown (Figure 3b). Since the ocean becomes more alkaline, the sensitivity of atmospheric CO_2 to the stronger soft-tissue pump is lowered, leading to slightly higher pCO_2 (by ~+2 ppm) than calculated from the isolated geochemical components: the "nonlinear CO_2 effect" (Figure 3c).

[31] This scenario is nearly identical to the one explored by *Marinov et al.* [2006], and the CO_2 sensitivity to the soft-tissue pump that they derive with a GCM is startlingly similar to our box model derived estimate (compare our Figures 3d and 3g with their Figure 2a). A linear approximation of the CO_2 sensitivity to the soft-tissue pump at today's ocean chemistry gives 13.3 ppm CO_2 drawdown per 0.1 μM regenerated [PO_4^{3-}] increase in good agreement with a GCM-based estimate [*Marinov et al.*, 2008] when corrected for their different soft-tissue stoichiometry. However, underlying the above changes is a ~6.4 fold increase in PAZ productivity, which violates evidence for lower Antarctic export production during the glacial [*Mortlock et al.*, 1991; *Kumar et al.*, 1993; *François et al.*, 1997; *Frank et al.*, 2000; *Kohfeld et al.*, 2005].

3.1.2. Reduced PAZ Deep Water Formation

[32] Now we consider reduced exchange between the PAZ and CDW, which represents the "stratification" hypothesis, broadly framed [*François et al.*, 1997]. We first assume that PAZ productivity decreases in step with gross nutrient input from CDW (i.e., a constant degree of nutrient consumption). Because CDW [PO_4^{3-}] does not change as a result of decreasing CDW/PAZ exchange under these conditions, PAZ [PO_4^{3-}] is also constant in this case (following the upper edge of the panels in Figure 3 from right to left). Atmospheric pCO_2 decreases by 36 ppm as surface-deep exchange approaches zero, the principle reason again being an increase in the global fraction of regenerated nutrients (P*,

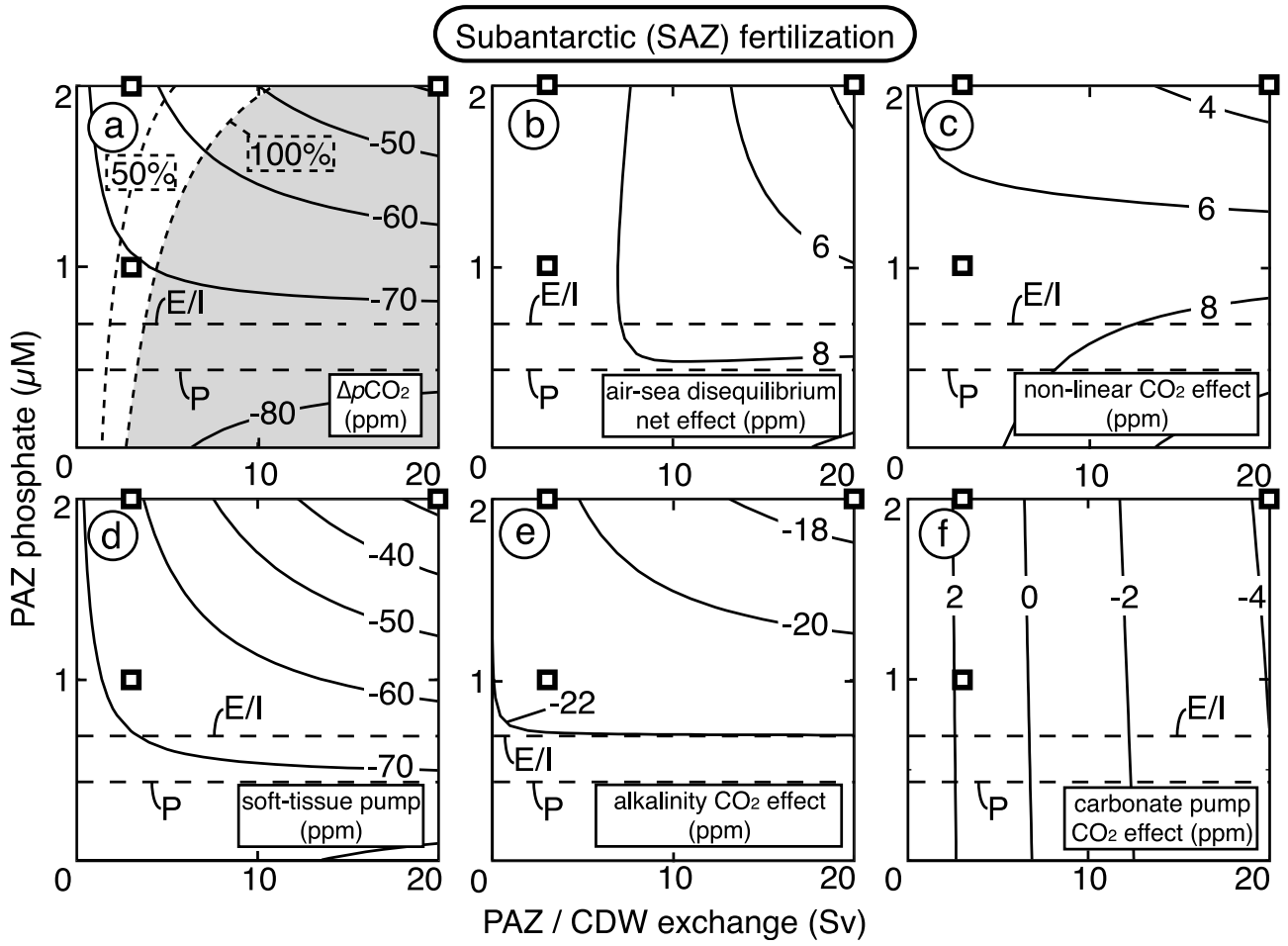

Figure 5. Model results for the polar Antarctic zone stratification experiment with enhanced subantarctic nutrient drawdown (see section 3.3). See captions for Figures 3 and 4.

Figure 3g), that is, a strengthening of the soft-tissue pump ($\Delta pCO_2 = -43$ ppm, Figure 3d). In contrast to the previous scenario, this CO_2 drawdown is achieved by reducing the fraction of ocean volume that is ventilated by the PAZ, which is highly inefficient in terms of the soft-tissue pump, and it occurs despite declining PAZ productivity.

[33] This decrease in deep ocean ventilation has a second, less broadly appreciated consequence: continued low-latitude rain and dissolution of calcium carbonate leads to a deep ocean buildup of regenerated alkalinity (Figure 3f). This corresponds to a strengthening of the carbonate pump, raising atmospheric CO_2 ($\Delta pCO_2 = +10$ ppm; Figures 3i and 3f). The sequestration of alkalinity in the deep ocean, moreover, makes these waters less corrosive to $CaCO_3$ rain, working against the influence of the strengthened soft-tissue pump, and thus curbs the dissolution-driven increase in whole ocean alkalinity ($\Delta pCO_2 = -5$ ppm) (Figures 3e and 3h).

[34] While the decrease in PAZ productivity is consistent with observations, there is a major concern here with observations regarding the ocean interior. A decrease in PAZ/CDW exchange in this or any other box model causes a greater fraction of the interior to be ventilated from the North Atlantic (Figure 7).

3.1.3. Combined Reductions in PAZ Nutrients and Deep Water Formation

[35] So far we have explored two scenarios, both achieving significant CO_2 drawdown but conflicting with ice age observations. We now explore a third scenario: decreased PAZ productivity coupled with an even greater decrease in gross nutrient supply by PAZ/CDW exchange, leading to a drop in PAZ $[PO_4^{3-}]$ (i.e., higher nutrient consumption). Given an 85% decrease in PAZ/CDW exchange (to 3 Sv) and a simultaneous 50% decrease in PAZ productivity (curved line labeled "50%" in Figure 3a), corresponding to a ~50% decrease in PAZ $[PO_4^{3-}]$ concentration (to 1μM), CO_2 decreases by 36 ppm. Again, the soft-tissue pump dominates this CO_2 change (−41 ppm), but in this case because of a combination of the PAZ becoming more efficient and less volumetrically important. As in the previous "stratification-only" scenario, the reduction of PAZ/CDW exchange prevents deep ocean regenerated alkalinity to come into contact with the atmosphere, a strengthening of the carbonate pump (+7 ppm). Again, the CO_2 effect of both

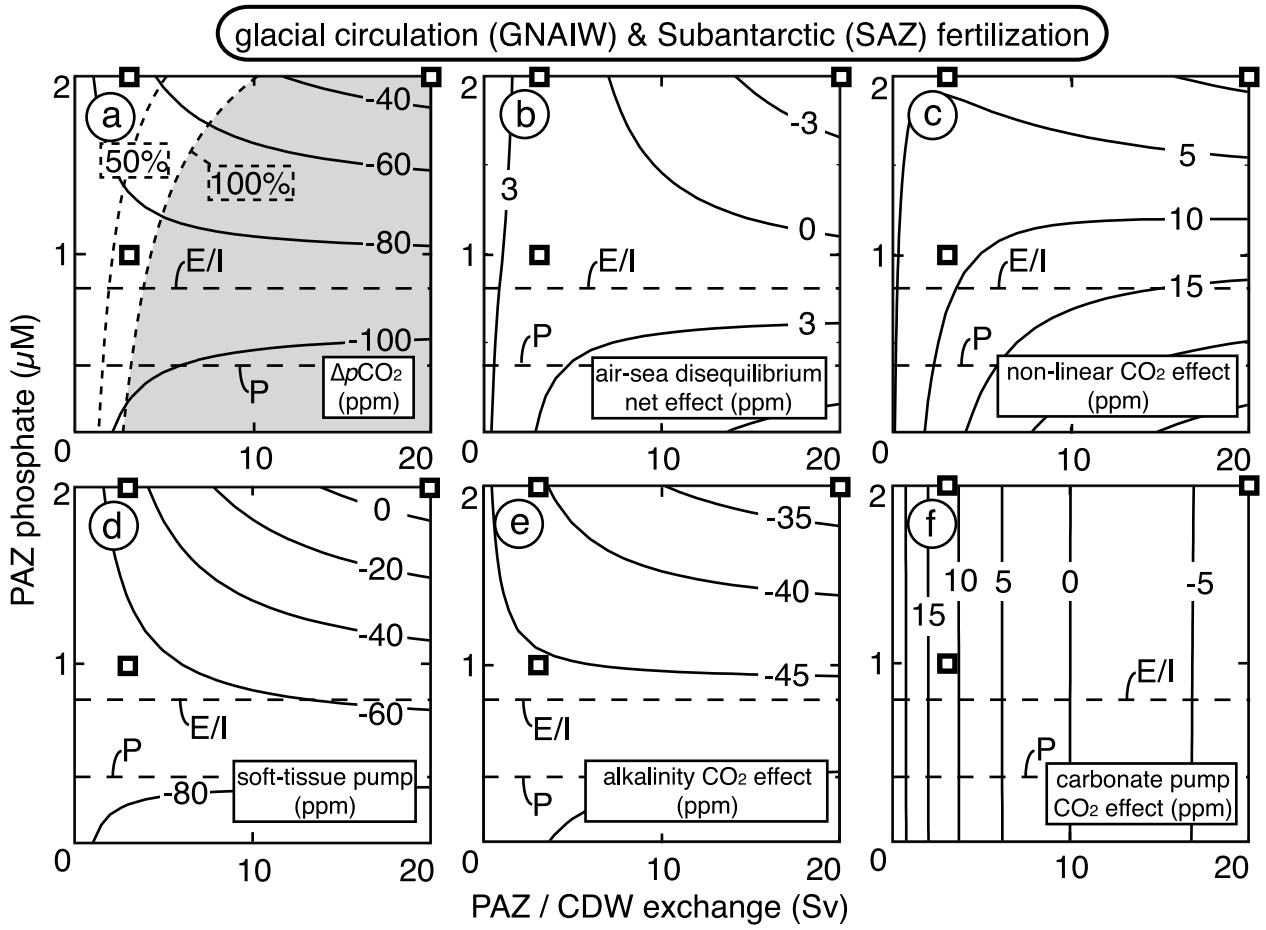

Figure 6. Model results for the polar Antarctic zone stratification experiment, conducted with glacial-like "GNAIW circulation" and enhanced subantarctic nutrient drawdown (see section 3.3). See captions for Figures 3 and 4.

soft-tissue and carbonate pump are being amplified (factor 7/6; Figure 8) by transient lysocline adjustments causing whole ocean alkalinity change (−5 ppm). Even for complete $[PO_4^{3-}]$ consumption at constant PAZ productivity, the atmospheric CO_2 decrease reaches only 44 ppm (Figure 3a).

3.1.4. PAZ CO_2 Gas-Exchange Reduction by Sea Ice Cover

[36] If the effective gas-exchange rate in the PAZ is reduced as a simple way to simulate the reduction in CO_2 due to sea ice expansion, the resulting decrease in atmospheric pCO_2 is essentially identical to a reduction in PAZ overturning (Figure S2a), reaching the maximal CO_2 effect of a complete cessation of deep ocean ventilation through the PAZ surface (i.e., no exchange between PAZ and CDW; [*Archer et al.*, 2003]). It follows that no combination of sea ice and stratification can exceed this maximal CO_2 drawdown of 36 ppm associated with PAZ barrier mechanisms [*Stephens and Keeling*, 2000] (Text S2); their CO_2 effects are not additive but rather compete for this finite CO_2 drawdown potential. In subsequent experiments, sea ice is not explicitly simulated, but the potential of complete sea ice cover to further lower CO_2 can be assessed from the pCO_2 difference between a given scenario and complete stratification (0 Sv PAZ/CDW exchange).

[37] The most important difference between PAZ stratification and sea ice–driven gas-exchange reduction involves the supply of nutrients to the surface ocean: only stratification decreases gross nutrient supply. As a result, a further decrease in CO_2 in the sea ice cover simulation due to greater surface nutrient drawdown would require an increase of PAZ productivity (gray shading in Figure S2a), which appears inconsistent with observations.

3.2. PAZ Changes Under Glacial Circulation

[38] The glacial circulation characterized by the formation of intermediate depth waters in the North Atlantic (GNAIW) leaves the deep ocean less well ventilated and thus prone to accumulation of both respired CO_2 and regenerated alkalinity. Also, interbasin (i.e., Atlantic-to-Indo-Pacific) gradients in the deep ocean set up by the ocean conveyor are relaxed. To assess the role of GNAIW formation and its relationship with the Antarctic stratification hypothesis, we focus our attention on (1) the NADW-to-GNAIW switch in isolation and (2) NADW-to-GNAIW switch

coupled to PAZ stratification and enhanced nutrient drawdown (3 Sv, 1 μM).

[39] Two opposing dynamics affect the soft-tissue pump in our GNAIW simulation. First, the abdication of the deep ocean by the North Atlantic leaves this voluminous body of water dominated by PAZ ventilation (Figure 7b) with the associated 2 μM burden of preformed [PO_4^{3-}], lowering the efficiency of the soft-tissue pump. Second, sequestration of nutrients in the isolated deep ocean depletes the mid-depth ocean ("nutrient deepening", [*Boyle*, 1988a, 1988b]), decreasing the burden of preformed [PO_4^{3-}] content of GNAIW by 50%, to 0.26 μM. In the absence of PAZ stratification, the first effect dominates, so that the soft-tissue pump works to raise CO_2 by 35 ppm (Figure 4d).

[40] The switch from NADW to GNAIW drives a transient dissolution event, primarily by allowing the higher-respired CO_2, more corrosive deep Indo-Pacific water to flood the deep North Atlantic [*Emerson and Archer*, 1992] but also by allowing respired CO_2 more time accumulate in the deep ocean before being brought up to the surface [*Boyle*, 1988a, 1988b]. Moreover, nutrient deepening starves low-latitude productivity, which decreases the $CaCO_3$ rain, raising whole ocean alkalinity through a deepening of the steady state lysocline [*Sigman et al.*, 1998]. As a result, whole ocean alkalinity rises so as to lower CO_2 (−14 ppm, Figure 4e), countering the weaker soft-tissue pump. The carbonate pump strength is roughly unchanged upon the switch from NADW to GNAIW (−1 ppm; Figure 4f), because of opposition between (1) reduced $CaCO_3$ rain onto the deep seafloor and (2) more time for regenerated alkalinity to accumulate in the deep ocean before brought up to the surface. In net, the GNAIW switch by itself raises CO_2 by 16 ppm (Figures 4a and 9).

[41] The above result suggests that GNAIW raises CO_2. But this is not the case in the context of the proposed Antarctic changes. If PAZ/CDW exchange is reduced to 3 Sv (−85%) and PAZ nutrient levels are decreased by 50% (to 1 μM [PO_4^{3-}]), both the volumetric importance and the preformed nutrient content of PAZ ventilated water decrease (Figure 7b), making the soft-tissue pump more efficient (−43 ppm instead of +35 ppm without PAZ stratification and nutrient drawdown; Figure 4d). However, this closing of the Southern Ocean leak of the biological pump also strengthens the carbonate pump by accumulating regenerated alkalinity in the deep ocean, raising CO_2 (+22 ppm, Figures 4f and 9b). The effect of the strengthened soft-tissue pump on deep ocean carbonate saturation, although partially offset by the stronger carbonate pump, makes the abyssal water more corrosive, and

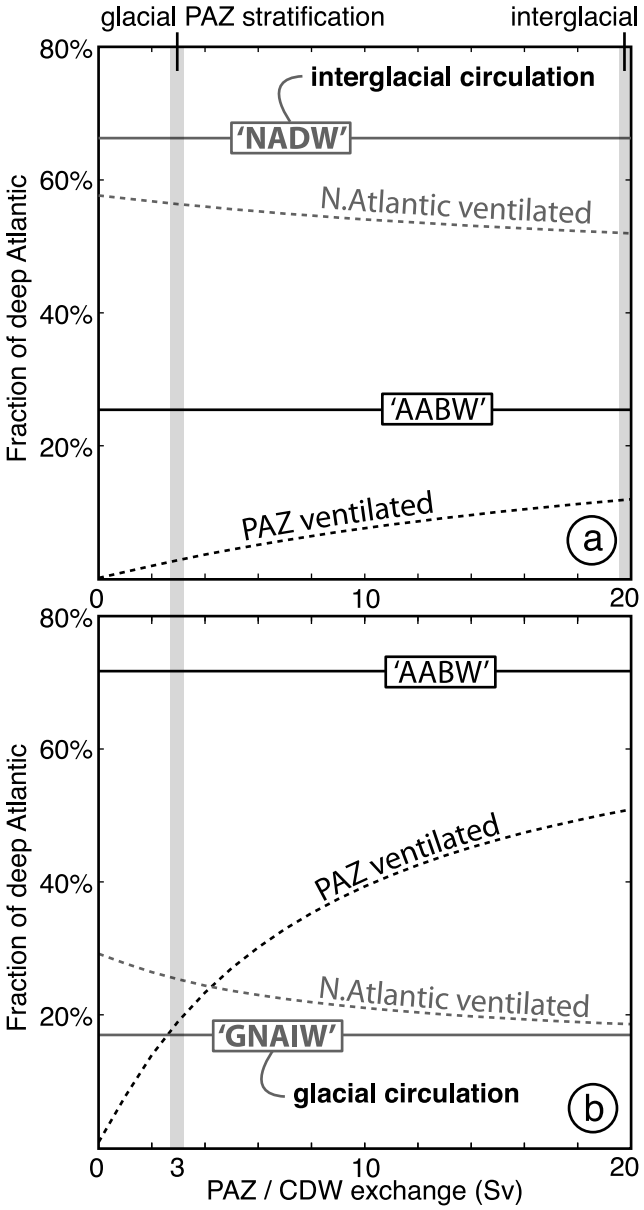

Figure 7. Simulated water masses and ventilation of the deep Atlantic box (>1500 m) for the (a) NADW-associated and (b) GNAIW-associated circulation. Ventilation is determined by two tracers set to 100% in the PAZ and North Atlantic (boreal) surface boxes, respectively, which are restored to zero in all other surface boxes. Water masses are determined by two tracers set to 100% in the northern component water box (NCW) and the circumpolar deep water (CDW) boxes, respectively, which are restored to zero in all surface boxes and the CDW/NCW box accordingly. Since there is no advective path in Figure 7b by which North Atlantic–sourced or North Atlantic–ventilated water reaches the deep Atlantic, it has been entirely mixed down from intermediate depth. In Figure 7b, the volume of North Atlantic–ventilated water in the deep Atlantic is greater than that of GNAIW-tagged water. This indicates that GNAIW-derived water enters the deep Southern Ocean without being ventilated in the Antarctic surface, after which it flows into the deep Atlantic box from the south. In the real ocean, GNAIW may have been entrained into the newly formed Antarctic-ventilated deep water as it sinks to the abyss along the Antarctic margin. This poorly studied process is a potentially important mechanism by which deep waters with low preformed nutrients might fill the deep ocean during glacial times, lowering CO_2 in the process [*Sigman et al.*, 2010].

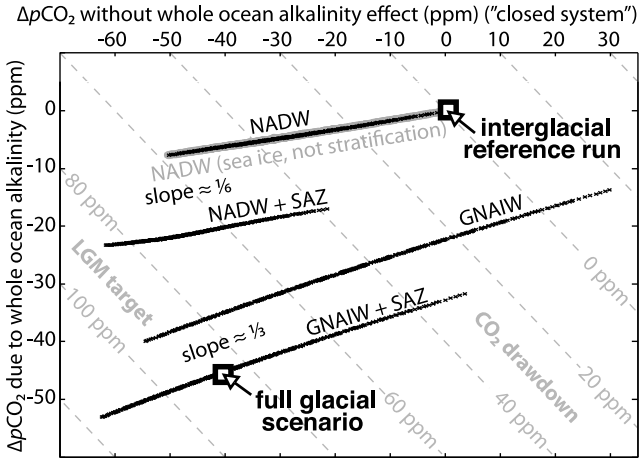

Figure 8. The whole ocean alkalinity component of the CO_2 change, plotted against atmospheric CO_2 without the whole ocean alkalinity component. Shown in black are all individual model runs contoured in Figures 3–6 (441 model runs in each experiment); in gray, behind the "NADW" experiment, are the "sea ice and nutrients" experiment results (see section 3.1.4 and Figure S2). Surprisingly, all model runs within one experiment plot on a common quasi-linear trend, although the soft-tissue and carbonate pumps are independent of one another, demonstrating that whole ocean alkalinity passively amplifies the combined CO_2 effect of the other geochemical mechanisms, by 16.5% or 32% depending on the circulation scheme (NADW or GNAIW). The gray contours indicate actual CO_2 levels achieved in the model runs.

carbonate compensation raises ocean alkalinity, further lowering CO_2 (−28 ppm, 15 ppm more drawdown then with GNAIW alone). Hence, GNAIW in conjunction with the Antarctic mechanisms lowers CO_2 by 48 ppm relative to the interglacial reference. This is greater than the 36 ppm CO_2 drawdown achieved by Antarctic stratification and greater nutrient consumption in the context of the NADW circulation (Figure 9a).

[42] Thus, the CO_2 impact of GNAIW depends critically on the status of the Antarctic. In isolation, it raises CO_2 by 16 ppm. However, when combined with the Antarctic stratification, it enhances the CO_2 drawdown by 12.9 ppm, a 28.7 ppm difference in net effect (Figure 9a). In this combined North Atlantic and Antarctic scenario, PAZ productivity is 40% lower than in the interglacial reference and thus satisfies the paleoproductivity evidence (Table 2).

[43] One conceptually important symptom of the CO_2 interaction between PAZ conditions and the NADW-to-GNAIW switch is that it has a profound effect on the CO_2 leverage of PAZ surface $[PO_4^{3-}]$ change in the context of PAZ stratification. With NADW, the cases of 2 and 0 μM $[PO_4^{3-}]$ in a PAZ surface with 3 Sv of overturning yield CO_2 levels that are 28 and 44 ppm lower than the interglacial case, respectively, a 16 ppm difference (Figure 3a). With GNAIW, the CO_2 reductions are 23 and 67 ppm, a 44 ppm difference (Figure 4a). This suggests that evidence for high degrees of LGM nutrient consumption in the PAZ surface are important for explaining the full amplitude of LGM CO_2 drawdown [*Robinson and Sigman*, 2008], a conclusion that might not have been reached if simulations were conducted with an NADW background circulation.

3.3. Glacial Subantarctic Nutrient Consumption

[44] Data and concepts support the hypothesis of higher degrees of nutrient consumption in the ice age sub-Antarctic as a result of natural iron fertilization [e.g., *Watson et al.* 2000; *R. S. Robinson et al.*, 2005; *Kohfeld et al.*, 2005; *Martinez-Garcia et al.*, 2009]. In our model, there are three mechanisms by which this would lower CO_2: (1) less preformed nutrients are fed from the sub-Antarctic into the mid-depth global ocean, increasing the efficiency of the soft-tissue pump; (2) lower nutrient concentration at mid-depth reduces low-latitude productivity and thus the $CaCO_3$ rain into the ocean interior, weakening the carbonate pump; and (3) the weaker carbonate pump and the stronger soft-tissue pump, as well as the reduced calcium carbonate rain in itself [*Keir*, 1988; *Sigman et al.*, 1998; *Matsumoto and Sarmiento*, 2008; *Loubere et al.*, 2004], would cause lysocline adjustments that render the whole ocean more alkaline (Figures 8 and 9b).

[45] Applying the subantarctic forcing in the absence of PAZ stratification (i.e., PAZ: 20 Sv, 2 μM), CO_2 is drawn down by 39 ppm (SAZ only in Figure 8a). The soft-tissue pump (−27 ppm, Figure 6d) and the whole ocean alkalinity effect (−17 ppm, Figure 6e) dominate, and the magnitude of CO_2 change is similar to previous estimates [*Watson et al.*, 2000; *R. S. Robinson et al.*, 2005; *Brovkin et al.*, 2007].

[46] In the context of NADW, the subantarctic nutrient drawdown acting alongside a stratified and lower-nutrient PAZ decreases atmospheric CO_2 by 35 ppm (Figure 5a) in addition to the 36 ppm drawdown achieved by the Antarctic mechanisms alone (Figure 3a). Net CO_2 interactions with PAZ changes and the NADW-to-GNAIW switch are minor although partitioned differently between the geochemical components (Table 2): in the context of GNAIW, the drawdown is 38 ppm (in addition to 48 ppm; Figure 4a). Thus, the subantarctic mechanism robustly lowers CO_2 by 35 to 40 ppm, irrespective of both GNAIW and Antarctic changes. However, this CO_2 decrease is reduced and a CO_2-reducing SAZ/GNAIW interaction arises when subantarctic $CaCO_3$ rain is included (Table S1 and Figure S1). Despite this caveat, the combination of the Antarctic mechanisms, GNAIW and the fertilized sub-Antarctic, in both rain ratio schemes, lowers CO_2 by the full amplitude of glacial/interglacial CO_2 variability (Figures 9 and S1). PAZ productivity in this scenario is 30% reduced, still in apparent agreement with the paleoproductivity proxies (Table 2).

4. Discussion

4.1. Mechanisms and Their Interactions

[47] Multiple Antarctic changes (nutrient status [e.g., *Sarmiento and Toggweiler*, 1984], stratification [*Toggweiler*, 1999] and sea ice cover [*Stephens and Keeling*, 2000]) have been studied with box models to understand their potential to explain low ice age CO_2. But how would these hypothesized changes interact with each

Table 2. Key Model Output for Selected Model Runs[a]

PAZ Forcing: Mixing/Phosphate (Sv/μM)	Case	CO_2 Change						Atl. $\Delta d^{13}C$: Interm.-Deep (per mil)	O_2 Utilization[b]		Deep $[CO_3^{2-}]$/ Lysocline			Ventilation Region			Productivity	
		ΔpCO_2 (ppm)	ΔST (ppm)	ΔCP (ppm)	ΔWOA (ppm)	ΔAS[e] (ppm)	ΔNLE[f] (ppm)		Interm. (μM)	Deep (μM)	Atlantic (μM)	N. Pacific (μM)	Low Lat.[c] (μM)	PAZ (%)	N. Atlantic (%)	SAZ (%)	Low Lat.[d] (%)	PAZ (%)
20/2	NADW	0	0	0	0	0	0	−0.15	177.9	164.7	107.2	76	85.8	24.3	23.0	32.3	100.0	100.0
20/2	GNAIW	15.8	35.4	−1.3	−13.7	−2.1	−2.6	0.67	130.1	141	103.2	86.1	94.4	44.0	12.1	25.9	80.0	131.0
20/2	SAZ	−38.8	−27	−4.2	−17	6.3	3.2	0.11	178.5	202.9	113.1	70.5	81.1	24.3	23.0	32.3	87.0	183.0
20/2	GNAIW+SAZ	−28.6	12.6	−6.4	−31.8	−1.9	−1.1	0.95	128	192.8	108.2	91.5	98.4	44.0	12.1	25.9	69.0	192.8
3/2	NADW	−26.9	−34.1	7.4	−3.7	4.3	−0.8	−0.14	193.2	207.4	112	74	84.6	5.7	32.0	38.6	100.0	15.0
3/2	GNAIW	−22.5	−21.5	22	−22.3	1.8	−2.6	0.91	149.1	207.3	104	87	94.4	16.5	17.9	39.0	80.0	20.0
3/2	SAZ	−63.6	−62	1.7	−20.7	11.8	5.6	0.12	196.4	252.9	117.8	67.7	79.3	5.7	32.0	38.6	87.0	27.5
3/2	GNAIW+SAZ	−67.4	−48.1	11.9	−40.8	5	4.6	1.21	150.5	248.4	109.3	92.7	98.22	16.5	17.9	39.0	69.0	28.9
3/1	NADW	−35.5	−41.3	7.4	−4.8	3.9	−0.7	−0.14	196.8	217.4	113.5	73.3	84.1	5.7	32.0	38.6	100.0	55.3
3/1	GNAIW	−48.4	−42.7	22.1	−28.3	2.2	−1.6	1.03	157.5	236.4	104.6	87.7	94.3	16.5	17.9	39.0	80.0	60.0
3/1	SAZ	−70.5	−68.2	1.8	−21.7	11.3	6.5	0.13	200.1	262.9	119.4	66.9	78.77	5.7	32.0	38.6	87.0	67.8
3/1	GNAIW+SAZ	−86.3	−66.7	11.9	−45.4	5.3	8.6	1.33	158.9	277.5	109.9	93.3	98.1	16.5	17.9	39.0	69.0	69.2

[a]The first (20/2; NADW) and the last experiment (3/1; GNAIW+SAZ) represent the interglacial reference and our best guess LGM scenario, respectively. A square marker in Figures 3 to 6 highlights the model runs shown here.
[b]Volumetrically averaged.
[c]Arithmetic mean for boxes with lysocline.
[d]Absolute export relative to reference.
[e] ΔAS, contribution from finite air-sea exchange, deviation from reference value (−2.7 ppm).
[f]ΔNLE, contribution of nonlinear effect to simulated CO_2 change.

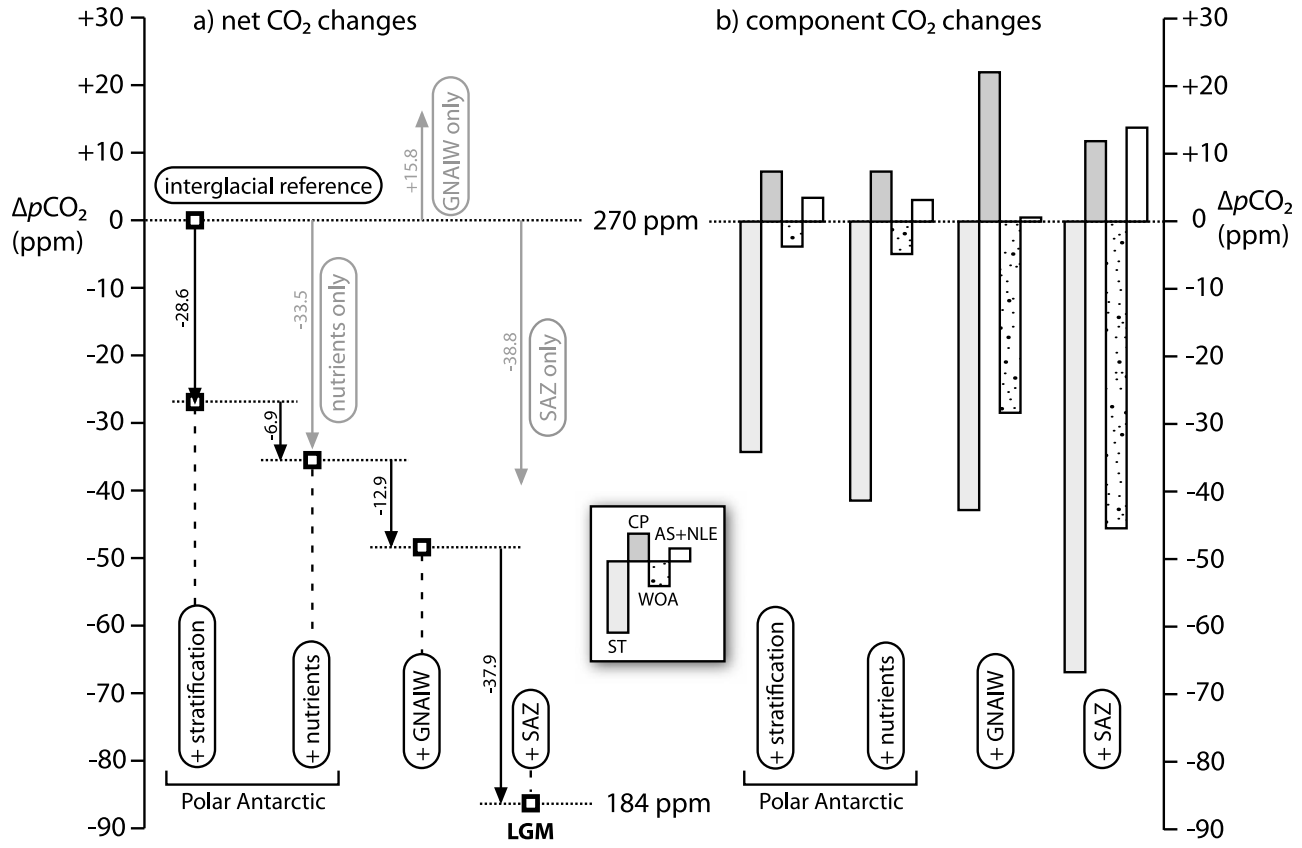

Figure 9. Summary of our model experiments. (a) The net CO_2 changes from the sequential implementation of the polar Antarctic, North Atlantic (GNAIW), and subantarctic (SAZ) mechanisms. The gray arrows indicate the CO_2 change caused by a given mechanism if implemented in isolation. (b) The contributions of the soft-tissue pump (ST), carbonate pump (CP), whole ocean alkalinity (WOA), air-sea disequilibrium (AS), and nonlinear effect (NLE) to the CO_2 change caused by the sequential implementation of the polar Antarctic, North Atlantic (GNAIW), and subantarctic (SAZ) mechanisms. We highlight here two observations: (1) the net CO_2 effect of the NADW-to-GNAIW switch depends on the state of the polar Antarctic (as shown in Figure 9a), and (2) the net CO_2 decreases caused by polar Antarctic stratification and the NADW-to-GNAIW switch are compromised by their strengthening of the carbonate pump (as shown in Figure 9b).

other and with other (e.g., North Atlantic) changes? Can we simply add up their CO_2 effects?

[48] As already pointed out by *Archer et al.* [2003], Antarctic sea ice and stratification are equivalent in their CO_2 effect, which stems from their role as a barrier to CO_2 evasion to the atmosphere, and thus they compete for a limited potential CO_2 reduction. In comparison, a change in Antarctic nutrient status in isolation has a greater maximum capacity to lower atmospheric CO_2 than either of the barrier mechanisms, partly because it can cause a greater decrease in the preformed nutrient concentration of the ocean interior and partly because its strengthening of the soft-tissue pump is not countered by strengthening of the carbonate pump. Greater Antarctic nutrient consumption can work with the barrier mechanisms to lower atmospheric CO_2. However, because Antarctic nutrient status affects Antarctic surface water pCO_2, the CO_2 drawdown capacity of the barrier mechanisms is usurped by an increase in Antarctic nutrient consumption, and vice versa. This highly nonlinear interaction limits the combined CO_2 drawdown in our simulations to $\leq$ 36 ppm, if ice age Antarctic productivity is not allowed to be higher than today. For illustration and to excuse our implicit treatment of the sea ice mechanism, if we add complete polar Antarctic sea ice cover to our full LGM scenario, only 3 ppm of additional CO_2 decline ensues (to a total of 89 ppm; compare to Figure 6). This does not discount the sea ice mechanism, which is very potent in isolation [e.g., *Stephens and Keeling*, 2000] and able to drive the entire Antarctic contribution to CO_2 reduction (i.e., $\sim$ 36 ppm) when areal coverage is near complete. Rather, this example highlights the importance of interactions among the Antarctic mechanisms.

[49] One reason that the Antarctic "barrier" mechanisms lower atmospheric CO_2 much less in our simulations than in previous studies [*Toggweiler*, 1999; *Stephens and Keeling*, 2000] is that both mechanisms sequester in the deep ocean not only respired CO_2 but also alkalinity from the dissolution of the $CaCO_3$ rain (see Text S2). In this way, the

barrier mechanisms strengthen the carbonate pump along with the soft-tissue pump, and the former counters the atmospheric CO_2 decline driven by the latter (Figure 9b). The concentration of regenerated alkalinity in our interglacial reference case (69 μM) matches the estimated global average of ~70 μM [*Sabine et al.* 2002; *Feely et al.*, 2002; *Chung et al.*, 2003], suggesting that our experiments are capturing an appropriate response strength for the carbonate pump. In contrast, *Toggweiler* [1999], by using the same regeneration profile for both $CaCO_3$ and organic carbon rain, and *Stephens and Keeling* [2000], having 35 μM regenerated alkalinity in their interglacial reference, do not adequately account for this effect and its amplification by whole ocean alkalinity (Figure 8 and Text S2). Hence, these studies circumvent the adverse effects of a carbonate pump strengthening and probably overestimate the potential for stratification or sea ice cover alone to draw down atmospheric CO_2.

[50] A weakness specific to Antarctic stratification is that it drastically reduces the fraction of the ocean ventilated through the Southern Ocean surface, at least in the context of box models (Figure 7 and Table 2). Although this makes the soft-tissue pump more effective and reduces Antarctic productivity as required by observations, it seems at odds with reconstructions of the main water masses of the glacial ocean, in particular in the Atlantic where southern sourced "AABW" dominated the basin below 2–2.5 km depth [e.g., *Rutberg et al.*, 2000; *Marchitto et al.*, 2002; *Curry and Oppo*, 2005; *Galbraith et al.*, 2007; *Lea and Boyle*, 1990]. The shift in deep ocean ventilation from partially Antarctic sourced to almost entirely non-Antarctic sourced is arguably the "dark secret" of many present box model experiments lowering CO_2 by a reduction in Antarctic overturning [e.g., *Toggweiler*, 1999; *Peacock et al.*, 2006].

[51] The ice age shoaling of North Atlantic overturning (i.e., the switch from NADW to GNAIW) has the potential to resolve this problem. The "GNAIW circulation" we employ to simulate peak glacial conditions increases the deep Atlantic volume ventilated by the PAZ ~4-fold relative to the "NADW circulation" stratification experiments. Under GNAIW conditions, even if the Antarctic is stratified (3 Sv), it still ventilates almost twice as much of the deep Atlantic as in the interglacial reference case (Figure 7). Moreover, if one traces northward and southward penetrating water rather than actual ventilation from specific polar surface boxes, the change from NADW to GNAIW mimics the observed dominance of "AABW" in the deep Atlantic (Figure 7). Nevertheless, we want to caution that entrainment of low preformed nutrient mid-depth water into the deep ocean does occur in our model, strengthening the soft-tissue pump. Along these lines, we want to stress that it is of great importance to develop approaches to distinguish between southern sourced and southern ventilated water, which become distinct with the onset of Antarctic stratification (Figure 7). An appropriate carbon isotope depth gradient arising in our full glacial simulation (Table 2) suggests that $\delta^{13}C$ observations in the LGM Atlantic [e.g., *Curry and Oppo*, 2005] may be interpreted as the result of "aging" rather then a difference in ventilation region.

[52] The second important set of CO_2 interactions that we document arises between GNAIW and the Antarctic mechanisms. We find that GNAIW obstructs the model's capacity to achieve the full glacial drawdown unless Antarctic changes, in particular enhanced nutrient drawdown, are considered as well. Previous studies that simulate stratification [e.g., *Toggweiler*, 1999; *Peacock et al.*, 2006] do not encounter the need for lower preformed nutrient content of glacial deep water ventilated in the Antarctic because they lower global preformed nutrient concentration by unrealistically shifting the direct ventilation of the abyss to the North Atlantic (see above). On the other hand, studies that simulate an appropriate change in Atlantic hydrography have come to the variable conclusion that GNAIW lowers [*Brovkin et al.*, 2007] or raises CO_2 [*Marinov et al.*, 2008]. We believe that this disagreement is a symptom of the interaction between GNAIW and the Antarctic mechanisms described herein: While *Marinov et al.* [2008] consider GNAIW in isolation, the *Brovkin et al.* [2007] study is characterized by an efficient Antarctic barrier for CO_2 (in their case sea ice rather than stratification).

[53] In contrast to GNAIW and the Antarctic mechanisms, nutrient drawdown in the subantarctic zone (SAZ) yields no net interaction with the other oceanographic drivers, contributing a CO_2 drawdown of 35 to 40 ppm. If we assume that the sub-Antarctic does produce and export $CaCO_3$ (not the standard case assumption), the CO_2 effect of subantarctic nutrient drawdown decreases, while an offsetting interaction with the NADW-to-GNAIW switch emerges (Table S1 and Figure S1). Because we suspect that increased nutrient drawdown would have increased $CaCO_3$ rain there and because CYCLOPS may overestimate the ocean volume ventilated by the glacial sub-Antarctic, we choose to think of our subantarctic CO_2 effect estimate as a upper bound. Overall, our simulations suggest that all mechanisms, including their interactions, are required to explain the lowest ice age CO_2 levels in a manner consistent with available oceanographic constraints.

4.2. Timing and pCO_2 During the Glacial

[54] The decline in atmospheric CO_2 during the progression of the last glacial cycle was apparently punctuated rather than gradual (Figure 1) [e.g., *Ahn and Brook*, 2008; *Petit et al.*, 1999; *Peacock et al.*, 2006]. In the spirit of *Peacock et al.* [2006], we propose a sequence of oceanographic changes that explains the first-order temporal pattern of CO_2 over the last glacial cycle without violating proxy evidence. The sudden drop in atmospheric CO_2 at the MIS 5e/d transition that is coincident with Antarctic cooling as recorded by ice core δD (~−40 ppm; Figure 1) may have been related to the onset of polar Antarctic stratification without the necessity for unsupported major changes in North Atlantic deep water formation at that time (−36 ppm; Figure 9), accompanied by some ocean cooling. The modeled CO_2 drawdown for stratification with an interglacial circulation is based almost entirely on a more efficient soft-tissue pump that may respond quickly to the onset of stratification.

[55] The second major shift in atmospheric CO_2 at the MIS 4/5 transition (~−35 ppm) [*Petit et al.*, 1999; *Ahn and*

Brook, 2008] may be related to natural subantarctic fertilization and a shift from NADW to GNAIW formation. The sediment records from the sub-Antarctic and the Atlantic basin support this suggestion, as inferred changes in subantarctic biogeochemistry and Atlantic hydrography appear to be broadly synchronous with CO_2 drawdown (Figure 1) [*Watson et al.*, 2000; *Hodell et al.*, 2003; *Kohfeld et al.*, 2005; *Martinez-Garcia et al.*, 2009]. We simulate these two changes acting along a stratified Antarctic to draw down CO_2 by ~50 ppm, much of which is achieved by an increase in whole ocean alkalinity (Figures 8 and 9). This role for whole ocean alkalinity is consistent with the finding that MIS 4 was characterized by the most severe dissolution event in the Atlantic over the last glacial cycle [*Crowley*, 1983]. Since the ocean's alkalinity inventory changes on a relatively long timescale, we find our model results roughly consistent with a slow CO_2 decline subsequent to the rapid MIS 5/4 drop.

[56] The dust flux, as recorded in ice cores, waned significantly for the duration of MIS 3 [*Petit et al.*, 1999] and so did the proposed iron fertilization [*Watson et al.*, 2000], which may explain the slightly higher but also variable pCO_2 levels of MIS 3 (~220 ppm; Figure 1). Reversion to NADW formation may also have occurred during MIS 3 (Figure 1) [*Martin and Lea*, 1998]. Indeed, a weakness of our interpretation is that we might have expected the atmospheric CO_2 concentration of stage 3 to increase more than observed, given the evidence for NADW formation and reduced dust input at that time. However, alkenone and diatom bound N isotope data suggest that MIS 3 was less distinct in the sub-Antarctic (Figure 1).

5. Conclusions

[57] Interactions among the oceanographic mechanisms of CO_2 change have caused much confusion when interpreting and comparing model results. Using a novel technique to parse the net CO_2 effects of these mechanisms into their geochemical components (soft-tissue pump, carbonate pump, whole ocean alkalinity, etc.), we establish a basis from which to assess the importance of the interactions among the mechanisms.

[58] Beginning with the polar Antarctic, in isolation, both stratification and sea ice–driven gas-exchange reduction can lower CO_2 by 36 ppm, and increased nutrient consumption can cause a 58 ppm decrease. However, when taken together as required by observations, these mechanisms are limited to 36 ppm. Were it not for the strengthening of the carbonate pump amplified by whole ocean alkalinity change, this decrease would have been 11 ppm greater.

[59] The other important interaction we document dominates the CO_2 effect caused by the ice age shoaling of North Atlantic overturning (i.e., the NADW-to-GNAIW switch). This switch makes the ocean more alkaline (lowering CO_2) but also tends to weaken the soft-tissue pump and strengthen the carbonate pump (both raising CO_2). Although GNAIW in isolation raises CO_2 by 16 ppm, its overlapping occurrence with the Antarctic mechanisms lowers CO_2 by 13 ppm. Thus, the 29 ppm GNAIW/Antarctic interaction is worth about a third of the total ice age CO_2 drawdown. Furthermore, it reconciles the opposite sense of CO_2 change caused by the NADW-to-GNAIW switch in the studies of *Brovkin et al.* [2007] versus *Marinov et al.* [2008]. Fertilization of the sub-Antarctic is the only mechanism we investigated that lacks a significant net interaction with the other drivers for low ice age CO_2 levels, unless subantarctic $CaCO_3$ rain is explicitly considered.

[60] Only the combination of all ocean mechanisms, including their interactions, permits our model to achieve the full amplitude of glacial/interglacial CO_2 change. This outcome contrasts with the results of *Toggweiler* [1999] and *Stephens and Keeling* [2000], who achieve much of the amplitude by Southern Ocean stratification and sea ice cover, respectively. While Toggweiler's study suffers from an unrealistic $CaCO_3$ regeneration scheme, Stephens and Keeling also appear to have too weak of a carbonate pump in their standard case, such that they will underestimate the carbonate pump increase upon Antarctic ice cover. Neither study would have achieved their full glacial CO_2 drawdown if they had an appropriate concentration of regenerated alkalinity, tracking the strength of the carbonate pump, in their interglacial reference model experiment. We find that including the carbonate pump in a model renders "nutrient deepening" [*Boyle*, 1988a, 1988b] and polar surface nutrient status more important, and Antarctic overturning and gas exchange less important, for achieving the ice age CO_2 reduction.

[61] Taking a step back, a general insight gained, central to the sensitivity of CO_2 to oceanographic changes and their interactions, is the importance of "ventilation volume", that is, the volume of the ocean ventilated through a given surface region: In any model, atmospheric CO_2 is essentially set by the pCO_2 of surface waters weighted by their ventilation volume. Along these lines, our model is successful in reaching the lowest ice age CO_2 levels only because it implicitly allows for the entrainment of mid-depth, subantarctic- and North Atlantic–ventilated water into the abyss; this is also the case in previous studies [e.g., *Toggweiler*, 1999; *Köhler et al.*, 2005; *Peacock et al.*, 2006]. Concerned about the physical oceanographic meaning of this solution, we suggest that resolving entrainment processes in the ocean interior, in particular along the Antarctic margin, is of central importance for the simulation of ice age CO_2 cycles.

[62] **Acknowledgment.** We thank J. R. Toggweiler for insightful discussion. Comments by two anonymous reviewers improved the manuscript. Support was provided by the US NSF, the German DFG, the Humboldt and MacArthur Foundations, the Siebel Energy Grand Challenge at Princeton, and O. Happel.

References

Ahn, J., and E. J. Brook (2008), Atmospheric CO_2 and climate on millennial time scales during the last glacial period, *Science*, *322*(5898), 83–85, doi:10.1126/science.1160832.

Anderson, L. A., and J. L. Sarmiento (1994), Redfield ratios of remineralization determined by nutrient data analysis, *Global Biogeochem. Cycles*, *8*(1), 65–80, doi:10.1029/93GB03318.

Archer, D. E., G. Eshel, A. Winguth, W. Broecker, R. Pierrehumbert, M. Tobis, and R. Jacob (2000), Atmospheric pCO_2 sensitivity to the biological pump in the ocean, *Global Biogeochem. Cycles*, *14*(4), 1219–1230, doi:10.1029/1999GB001216.

Archer, D. E., P. A. Martin, J. Milovich, V. Brovkin, G. K. Plattner, and C. Ashendel (2003), Model sensitivity in the effect of Antarctic sea ice and stratification on atmospheric pCO_2, *Paleoceanography*, *18*(1), 1012, doi:10.1029/2002PA000760.

Berelson, W. M. (2001), The flux of particulate organic carbon into the ocean interior: A comparison of four U.S. JGOFS regional studies, *Oceanography*, *14*(4), 59–67.

Boyle, E. A. (1988a), Vertical oceanic nutrient fractionation and glacial interglacial CO_2 cycles, *Nature*, *331*(6151), 55–56, doi:10.1038/331055a0.

Boyle, E. A. (1988b), The role of vertical chemical fractionation in controlling late Quaternary atmospheric carbon dioxide, *J. Geophys. Res.*, *93*(C12), 15,701–15,714, doi:10.1029/JC093iC12p15701.

Boyle, E. A., and L. D. Keigwin (1982), Deep circulation of the North Atlantic over the last 200,000 years: Geochemical evidence, *Science*, *218*(4574), 784–787, doi:10.1126/science.218.4574.784.

Boyle, E. A., and L. Keigwin (1987), North Atlantic thermohaline circulation during the past 20,000 years linked to high-latitude surface temperature, *Nature*, *330*(6143), 35–40, doi:10.1038/330035a0.

Boyle, E. A., L. Labeyrie, and J. C. Duplessy (1995), Calcitic foraminiferal data confirmed by cadmium in aragonitic Hoeglundina: Application to the Last Glacial Maximum in the northern Indian Ocean, *Paleoceanography*, *10*(5), 881–900, doi:10.1029/95PA01625.

Broecker, W. S., and T.-H. Peng (1987), The role of $CaCO_3$ compensation in the glacial to interglacial atmospheric CO_2 change, *Global Biogeochem. Cycles*, *1*(1), 15–29, doi:10.1029/GB001i001p00015.

Broecker, W. S., and T.-H. Peng (1989), The cause of the glacial to interglacial atmospheric CO_2 change: A polar alkalinity hypothesis, *Paleoceanography*, *3*(3), 215–239.

Brovkin, V., A. Ganopolski, D. Archer, and S. Rahmstorf (2007), Lowering of glacial atmospheric CO_2 in response to changes in oceanic circulation and marine biogeochemistry, *Paleoceanography*, *22*, PA4202, doi:10.1029/2006PA001380.

Chung, S. N., K. Lee, R. A. Feely, C. L. Sabine, F. J. Millero, R. Wanninkhof, J. L. Bullister, R. M. Key, and T. H. Peng (2003), Calcium carbonate budget in the Atlantic Ocean based on water column inorganic carbon chemistry, *Global Biogeochem. Cycles*, *17*(4), 1093, doi:10.1029/2002GB002001.

Crosta, X., and A. Shemesh (2002), Reconciling down core anticorrelation of diatom carbon and nitrogen isotopic ratios from the Southern Ocean, *Paleoceanography*, *17*(1), 1010, doi:10.1029/2000PA000565.

Crowley, T. J. (1983), Calcium-carbonate preservation patterns in the central North Atlantic during the last 150,000 years, *Mar. Geol.*, *51*(1–2), 1–14, doi:10.1016/0025-3227(83)90085-3.

Curry, W. B., and D. W. Oppo (2005), Glacial water mass geometry and the distribution of $\delta^{13}C$ of Sigma CO_2 in the western Atlantic Ocean, *Paleoceanography*, *20*, PA1017, doi:10.1029/2004PA001021.

De La Rocha, C. L. (2006), Opal-based isotopic proxies of paleoenvironmental conditions, *Global Biogeochem. Cycles*, *20*, GB4S09, doi:10.1029/2005GB002664.

De La Rocha, C. L., M. A. Brzezinski, M. J. DeNiro, and A. Shemesh (1998), Silicon-isotope composition of diatoms as an indicator of past oceanic change, *Nature*, *395*(6703), 680–683, doi:10.1038/27174.

Duplessy, J. C., N. J. Shackleton, R. K. Matthews, W. Prell, W. F. Ruddiman, M. Caralp, and C. H. Hendy (1984), ^{13}C record of benthic foraminifera in the last interglacial ocean–implications for the carbon-cycle and the global deep-water circulation, *Quat. Res.*, *21*(2), 225–243, doi:10.1016/0033-5894(84)90099-1.

Duplessy, J. C., N. J. Shackleton, R. G. Fairbanks, L. Labeyrie, D. Oppo, and N. Kallel (1988), Deepwater source variations during the last climatic cycle and their impact on the global deepwater circulation, *Paleoceanography*, *3*(3), 343–360, doi:10.1029/PA003i003p00343.

Elderfield, H., and R. E. M. Rickaby (2000), Oceanic Cd/P ratio and nutrient utilization in the glacial Southern Ocean, *Nature*, *405*(6784), 305–310, doi:10.1038/35012507.

Emerson, S., and D. Archer (1992), Glacial carbonate dissolution cycles and atmospheric pCO_2: A view from the ocean bottom, *Paleoceanography*, *7*(3), 319–331, doi:10.1029/92PA00773.

Feely, R. A., et al. (2002), In situ calcium carbonate dissolution in the Pacific Ocean, *Global Biogeochem. Cycles*, *16*(4), 1144, doi:10.1029/2002GB001866.

François, R., M. A. Altabet, E. F. Yu, D. M. Sigman, M. P. Bacon, M. Frank, G. Bohrmann, G. Bareille, and L. D. Labeyrie (1997), Contribution of Southern Ocean surface-water stratification to low atmospheric CO_2 concentrations during the last glacial period, *Nature*, *389*(6654), 929–935, doi:10.1038/40073.

Frank, M., R. Gersonde, M. R. van der Loeff, G. Bohrmann, C. C. Nurnberg, P. W. Kubik, M. Suter, and A. Mangini (2000), Similar glacial and interglacial export bioproductivity in the Atlantic sector of the Southern Ocean: Multiproxy evidence and implications for glacial atmospheric CO_2, *Paleoceanography*, *15*(6), 642–658, doi:10.1029/2000PA000497.

Galbraith, E. D., S. L. Jaccard, T. F. Pedersen, D. M. Sigman, G. H. Haug, M. Cook, J. R. Southon, and R. Francois (2007), Carbon dioxide release from the North Pacific abyss during the last deglaciation, *Nature*, *449*, 890–893, doi:10.1038/nature06227.

Gherardi, J. M., L. Labeyrie, S. Nave, R. Francois, J. F. McManus, and E. Cortijo (2009), Glacial-interglacial circulation changes inferred from $^{231}Pa/^{230}Th$ sedimentary record in the North Atlantic region, *Paleoceanography*, *24*, PA2204, doi:10.1029/2008PA001696.

Herguera, J. C. (1992), Deep-sea benthic foraminifera and biogenic opal–Glacial to postglacial productivity changes in the western equatorial Pacific, *Mar. Micropaleontol.*, *19*(1–2), 79–98, doi:10.1016/0377-8398(92)90022-C.

Hodell, D. A., K. A. Venz, C. D. Charles, and U. S. Ninnemann (2003), Pleistocene vertical carbon isotope and carbonate gradients in the South Atlantic sector of the Southern Ocean, *Geochem. Geophys. Geosyst.*, *4*(1), 1004, doi:10.1029/2002GC000367.

Honjo, S. (2004), Particle export and the biological pump in the Southern Ocean, *Antarct. Sci.*, *16*(4), 501–516.

Ito, T., and M. J. Follows (2005), Preformed phosphate, soft tissue pump and atmospheric CO_2, *J. Mar. Res.*, *63*(4), 813–839, doi:10.1357/0022240054663231.

Kallel, N., L. D. Labeyrie, A. Juillet-Leclerc, and J. C. Duplessy (1988), A deep hydrological front between intermediate and deep-water masses in the glacial Indian Ocean, *Nature*, *333*(6174), 651–655, doi:10.1038/333651a0.

Keigwin, L. D. (1998), Glacial-age hydrography of the far northwest Pacific Ocean, *Paleoceanography*, *13*(4), 323–339, doi:10.1029/98PA00874.

Keigwin, L. D., and E. A. Boyle (1989), Late Quaternary paleochemistry of high-latitude surface waters, *Palaeogeogr. Palaeoclimatol. Palaeoecol.*, *73*(1–2), 85–106, doi:10.1016/0031-0182(89)90047-3.

Keir, R. S. (1988), On the Late Pleistocene ocean geochemistry and circulation, *Paleoceanography*, *3*(4), 413–445, doi:10.1029/PA003i004p00413.

Klaas, C., and D. E. Archer (2002), Association of sinking organic matter with various types of mineral ballast in the deep sea: Implications for the rain ratio, *Global Biogeochem. Cycles*, *16*(4), 1116, doi:10.1029/2001GB001765.

Kohfeld, K. E., C. Le Quere, S. P. Harrison, and R. F. Anderson (2005), Role of marine biology in glacial-interglacial CO_2 cycles, *Science*, *308*(5718), 74–78, doi:10.1126/science.1105375.

Köhler, P., H. Fischer, G. Munhoven, and R. E. Zeebe (2005), Quantitative interpretation of atmospheric carbon records over the last glacial termination, *Global Biogeochem. Cycles*, *19*, GB4020, doi:10.1029/2004GB002345.

Kumar, N., R. Gwiazda, R. F. Anderson, and P. N. Froelich (1993), $^{231}Pa/^{230}Th$ ratios in sediments as a proxy for past changes in Southern Ocean productivity, *Nature*, *362*(6415), 45–48, doi:10.1038/362045a0.

Kumar, N., R. F. Anderson, R. A. Mortlock, P. N. Froelich, P. Kubik, B. Dittrichhannen, and M. Suter (1995), Increased biological productivity and export production in the glacial Southern Ocean, *Nature*, *378*(6558), 675–680, doi:10.1038/378675a0.

Kwon, E. Y., and F. Primeau (2008), Optimization and sensitivity of a global biogeochemistry ocean model using combined in situ DIC, alkalinity, and phosphate data, *J. Geophys. Res.*, *113*, C08011, doi:10.1029/2007JC004520.

Lea, D. W., and E. A. Boyle (1990), A 210,000-year record of barium variability in the deep northwest Atlantic Ocean, *Nature*, *347*(6290), 269–272, doi:10.1038/347269a0.

Lisiecki, L. E., and M. E. Raymo (2005), A Pliocene-Pleistocene stack of 57 globally distributed benthic $\delta^{18}O$ records, *Paleoceanography*, *20*, PA1003, doi:10.1029/2004PA001071.

Loubere, P., F. Mekik, R. Francois, and S. Pichat (2004), Export fluxes of calcite in the eastern equatorial Pacific from the Last Glacial Maximum to present, *Paleoceanography*, *19*, PA2018, doi:10.1029/2003PA000986.

Lynch-Stieglitz, J., et al. (2007), Atlantic meridional overturning circulation during the Last Glacial Maximum, *Science*, *316*(5821), 66–69, doi:10.1126/science.1137127.

Marchitto, T. M., D. W. Oppo, and W. B. Curry (2002), Paired benthic foraminiferal Cd/Ca and Zn/Ca evidence for a greatly increased presence

of Southern Ocean Water in the glacial North Atlantic, *Paleoceanography*, *17*(3),1038, doi:10.1029/2000PA000598.

Marinov, I., A. Gnanadesikan, J. R. Toggweiler, and J. L. Sarmiento (2006), The Southern Ocean biogeochemical divide, *Nature*, *441*(7096), 964–967, doi:10.1038/nature04883.

Marinov, I., A. Gnanadesikan, J. L. Sarmiento, J. R. Toggweiler, M. Follows, and B. K. Mignone (2008), Impact of oceanic circulation on biological carbon storage in the ocean and atmospheric pCO_2, *Global Biogeochem. Cycles*, *22*, GB3007, doi:10.1029/2007GB002958.

Martin, J. H. (1990), Glacial-interglacial CO_2 change: The iron hypothesis, *Paleoceanography*, *5*(1), 1–13, doi:10.1029/PA005i001p00001.

Martin, P. A., and D. W. Lea (1998), Comparison of water mass changes in the deep tropical Atlantic derived from Cd/Ca and carbon isotope records: Implications for changing Ba composition of deep Atlantic water masses, *Paleoceanography*, *13*(6), 572–585, doi:10.1029/98PA02670.

Martinez-Garcia, A., A. Rosell-Mele, W. Geibert, R. Gersonde, P. Masque, V. Gaspari, and C. Barbante (2009), Links between iron supply, marine productivity, sea surface temperature, and CO_2 over the last 1.1 Ma, *Paleoceanography*, *24*, PA1207, doi:10.1029/2008PA001657.

Mashiotta, T. A., D. W. Lea, and H. J. Spero (1997), Experimental determination of cadmium uptake in shells of the planktonic foraminifera Orbulina universa and Globigerina bulloides: Implications for surface water paleoreconstructions, *Geochim. Cosmochim. Acta*, *61*(19), 4053–4065, doi:10.1016/S0016-7037(97)00206-8.

Matsumoto, K., and J. Lynch-Stieglitz (1999), Similar glacial and Holocene deep water circulation inferred from southeast Pacific benthic foraminiferal carbon isotope composition, *Paleoceanography*, *14*(2), 149–163, doi:10.1029/1998PA900028.

Matsumoto, K., and J. L. Sarmiento (2008), A corollary to the silicic acid leakage hypothesis, *Paleoceanography*, *23*, PA2203, doi:10.1029/2007PA001515.

Matsumoto, K., T. Oba, J. Lynch-Stieglitz, and H. Yamamoto (2002), Interior hydrography and circulation of the glacial Pacific Ocean, *Quat. Sci. Rev.*, *21*(14–15), 1693–1704, doi:10.1016/S0277-3791(01)00142-1.

McManus, J. F., R. Francois, J. M. Gherardi, L. D. Keigwin, and S. Brown-Leger (2004), Collapse and rapid resumption of Atlantic meridional circulation linked to deglacial climate changes, *Nature*, *428*(6985), 834–837, doi:10.1038/nature02494.

Mortlock, R. A., C. D. Charles, P. N. Froelich, M. A. Zibello, J. Saltzman, J. D. Hays, and L. H. Burckle (1991), Evidence for lower productivity in the Antarctic ocean during the last glaciation, *Nature*, *351*(6323), 220–223, doi:10.1038/351220a0.

Oppo, D. W., M. E. Raymo, G. P. Lohmann, A. C. Mix, J. D. Wright, and W. L. Prell (1995), A $\delta^{13}C$ record of Upper North Atlantic deep water during the past 2.6 million years, *Paleoceanography*, *10*(3), 373–394, doi:10.1029/95PA00332.

Peacock, S., E. Lane, and J. M. Restrepo (2006), A possible sequence of events for the generalized glacial-interglacial cycle, *Global Biogeochem. Cycles*, *20*, GB2010, doi:10.1029/2005GB002448.

Petit, J. R., et al. (1999), Climate and atmospheric history of the past 420,000 years from the Vostok ice core, Antarctica, *Nature*, *399*(6735), 429–436, doi:10.1038/20859.

Robinson, L. F., J. F. Adkins, L. D. Keigwin, J. Southon, D. P. Fernandez, S. L. Wang, and D. S. Scheirer (2005), Radiocarbon variability in the western North Atlantic during the last deglaciation, *Science*, *310*(5753), 1469–1473, doi:10.1126/science.1114832.

Robinson, R. S., and D. M. Sigman (2008), Nitrogen isotopic evidence for a poleward decrease in surface nitrate within the ice age Antarctic, *Quat. Sci. Rev.*, *27*(9–10), 1076–1090, doi:10.1016/j.quascirev.2008.02.005.

Robinson, R. S., B. G. Brunelle, and D. M. Sigman (2004), Revisiting nutrient utilization in the glacial Antarctic: Evidence from a new method for diatom-bound N isotopic analysis, *Paleoceanography*, *19*, PA3001, doi:10.1029/2003PA000996.

Robinson, R. S., D. M. Sigman, P. J. DiFiore, M. M. Rohde, T. A. Mashiotta, and D. W. Lea (2005), Diatom-bound $^{15}N/^{14}N$: New support for enhanced nutrient consumption in the ice age subantarctic, *Paleoceanography*, *20*, PA3003, doi:10.1029/2004PA001114.

Rosenthal, Y., E. A. Boyle, and L. Labeyrie (1997), Last glacial maximum paleochemistry and deepwater circulation in the Southern Ocean: Evidence from foraminiferal cadmium, *Paleoceanography*, *12*(6), 787–796, doi:10.1029/97PA02508.

Rosenthal, Y., M. Dahan, and A. Shemesh (2000), Southern Ocean contributions to glacial-interglacial changes of atmospheric pCO_2: An assessment of carbon isotope records in diatoms, *Paleoceanography*, *15*(1), 65–75, doi:10.1029/1999PA000369.

Rutberg, R. L., S. R. Hemming, and S. L. Goldstein (2000), Reduced North Atlantic deep water flux to the glacial Southern Ocean inferred from neodymium isotope ratios, *Nature*, *405*(6789), 935–938, doi:10.1038/35016049.

Sabine, C. L., R. M. Key, R. A. Feely, and D. Greeley (2002), Inorganic carbon in the Indian Ocean: Distribution and dissolution processes, *Global Biogeochem. Cycles*, *16*(4), 1067, doi:10.1029/2002GB001869.

Sarmiento, J. L., and J. R. Toggweiler (1984), A new model for the role of the oceans in determining atmospheric pCO_2, *Nature*, *308*(5960), 621–624, doi:10.1038/308621a0.

Sarmiento, J. L., J. Dunne, A. Gnanadesikan, R. M. Key, K. Matsumoto, and R. Slater (2002), A new estimate of the $CaCO_3$ to organic carbon export ratio, *Global Biogeochem. Cycles*, *16*(4), 1107, doi:10.1029/2002GB001919.

Sarmiento, J. L., N. Gruber, M. A. Brzezinski, and J. P. Dunne (2004), High-latitude controls of thermocline nutrients and low latitude biological productivity, *Nature*, *427*(6969), 56–60, doi:10.1038/nature02127.

Shackleton, N. J., M. A. Hall, and E. Vincent (2000), Phase relationships between millennial-scale events 64,000–24,000 years ago, *Paleoceanography*, *15*(6), 565–569, doi:10.1029/2000PA000513.

Sigman, D. M., and E. A. Boyle (2000), Glacial/interglacial variations in atmospheric carbon dioxide, *Nature*, *407*(6806), 859–869, doi:10.1038/35038000.

Sigman, D. M., and G. H. Haug (2003), The biological pump in the past, in *Treatise on Geochemistry*, vol. 6, edited by H. Elderfield, H. D. Holland, and K. K. Turekian, pp. 491–528, Elsevier, New York, ISBN:0-08-043751-6.

Sigman, D. M., D. C. McCorkle, and W. R. Martin (1998), The calcite lysocline as a constraint on glacial/interglacial low-latitude production changes, *Global Biogeochem. Cycles*, *12*(3), 409–427, doi:10.1029/98GB01184.

Sigman, D. M., M. A. Altabet, R. Francois, D. C. McCorkle, and J. F. Gaillard (1999), The isotopic composition of diatom-bound nitrogen in Southern Ocean sediments, *Paleoceanography*, *14*(2), 118–134, doi:10.1029/1998PA900018.

Sigman, D. M., S. J. Lehman, and D. W. Oppo (2003), Evaluating mechanisms of nutrient depletion and ^{13}C enrichment in the intermediate-depth Atlantic during the last ice age, *Paleoceanography*, *18*(3), 1072, doi:10.1029/2002PA000818.

Sigman, D. M., P. J. DiFiore, M. P. Hain, C. Deutsch, Y. Wang, D. M. Karl, A. N. Knapp, M. F. Lehmann, and S. Pantoja (2009), The dual isotopes of deep nitrate as a constraint on the cycle and budget of oceanic fixed nitrogen, *Deep Sea Res., Part I*, *56*(9), 1419–1439, doi:10.1016/j.dsr.2009.04.007.

Sigman, D. M., M. P. Hain, and G. H. Haug (2010), The polar ocean and glacial cycles in atmospheric CO_2 concentration, *Nature*, *466*(7302), 47–55, doi:10.1038/nature09149.

Stephens, B. B., and R. F. Keeling (2000), The influence of Antarctic sea ice on glacial-interglacial CO_2 variations, *Nature*, *404*(6774), 171–174, doi:10.1038/35004556.

Toggweiler, J. R. (1999), Variation of atmospheric CO_2 by ventilation of the ocean's deepest water, *Paleoceanography*, *14*(5), 571–588, doi:10.1029/1999PA900033.

Toggweiler, J. R., K. Dixon, and W. S. Broecker (1991), The Peru upwelling and the ventilation of the South Pacific thermocline, *J. Geophys. Res.*, *96*(C11), 20,467–20,497, doi:10.1029/91JC02063.

Toggweiler, J. R., A. Gnanadesikan, S. Carson, R. Murnane, and J. L. Sarmiento (2003), Representation of the carbon cycle in box models and GCMs: 1. Solubility pump, *Global Biogeochem. Cycles*, *17*(1), 1026, doi:10.1029/2001GB001401.

Watson, A. J., D. C. E. Bakker, A. J. Ridgwell, P. W. Boyd, and C. S. Law (2000), Effect of iron supply on Southern Ocean CO_2 uptake and implications for glacial atmospheric CO_2, *Nature*, *407*(6805), 730–733, doi:10.1038/35037561.

Yu, E. F., R. Francois, and M. P. Bacon (1996), Similar rates of modern and last-glacial ocean thermohaline circulation inferred from radiochemical data, *Nature*, *379*(6567), 689–694, doi:10.1038/379689a0.

M. P. Hain and D. M. Sigman, Department of Geosciences, Princeton University, Guyot Hall, Princeton, NJ 08544-1013, USA. (mhain@princeton.edu)

G. H. Haug, Geological Institute, Department of Earth Sciences, ETH Zürich, Sonneggstr. 5, Zürich CH-8092, Switzerland.